

# Gravitational waves from the Axiverse

---

**Saurav Das,<sup>a</sup> Francesc Ferrer<sup>a</sup>**

<sup>a</sup>*Department of Physics and McDonnell Center for the Space Sciences, Washington University, St. Louis, Missouri 63130, USA*

*E-mail:* [s.das@wustl.edu](mailto:s.das@wustl.edu), [ferrer@wustl.edu](mailto:ferrer@wustl.edu)

ABSTRACT: Models with axion like particles (ALPs) often predict the formation of a string-domain wall network in the early universe. We study how such networks of defects appear in the context of string theory, and discuss the conditions for their long-term stability. In a scenario with several axions, we show how a bias term in the potential arises naturally from the effects of multiple instantons, leading to the eventual decay of the domain walls. We find that the annihilation of the network leads to the generation of a stochastic gravitational wave background (SGWB) with a spectrum that has characteristic contributions from both walls and strings. The unique shape of the spectrum provides an opportunity to probe string theory axions at existing and upcoming observatories. The extinction of the network is also accompanied by the production of different axion mass eigenstates. In a region of the parameter space, the lightest eigenstate can be long lived and make up the dark matter in the universe.

---

## Contents

<b>1</b>	<b>Introduction</b>	<b>1</b>
<b>2</b>	<b>Domain walls of string theory axions</b>	<b>3</b>
<b>3</b>	<b>Evolution and decay of the string-domain wall network</b>	<b>5</b>
3.1	Size of the bias term	8
<b>4</b>	<b>Phenomenological signatures</b>	<b>8</b>
4.1	Production of Gravitational waves	9
4.1.1	Gravitational waves from domain walls	9
4.1.2	Gravitational waves from strings in the scaling regime	11
4.2	Production of axion dark matter	13
4.2.1	Axions from the collapse of domain walls	17
4.2.2	Axions from the misalignment mechanism	19
4.2.3	Axion emission from strings in the scaling regime	20
<b>5</b>	<b>Conclusions</b>	<b>22</b>
<b>A</b>	<b>Condition on the charges</b>	<b>24</b>
<b>B</b>	<b>Role of unequal initial abundance of vacua</b>	<b>24</b>
<b>C</b>	<b>GWs from decays during an early matter dominated era</b>	<b>25</b>
<b>D</b>	<b>Averaged misalignment angle</b>	<b>26</b>
<b>E</b>	<b>No EMD from string network decay during scaling</b>	<b>26</b>
<b>F</b>	<b>Dark matter abundance from EMD</b>	<b>27</b>

---

## 1 Introduction

One of the most general low energy predictions of string theory is the presence of multiple axions [1–5]. In this context, the four-dimensional axions are realized as the zero modes of higher dimensional gauge fields. A linear combination of these fields can couple to Quantum Chromodynamics (QCD) in the way required to solve the strong CP problem [6–8], similar to the Peccei-Quinn (PQ) axion [9–12]. Furthermore, the fact that the masses of string

theory axions are generated only from non-perturbative effects is generically expected to ameliorate [13] the quality problem of the field theory PQ axion [14–19].

In string theory compactifications, the QCD axion is generally accompanied by a plethora of other light axionic fields with their own interesting dynamics [20–23]. In particular, the axions could be magnetically sourced by string theory axion strings that are expected to be present in specific models of brane inflation [24–27]. Much like field theory axions, the dynamics of string theory axions in many axiverse constructions is described by a potential generated from non-perturbative instanton effects [28, 29]. Thus, the 4D effective field theory (EFT) of the multiple axionic fields can then be written as:

$$\mathcal{L} \supset -\frac{K_{ij}}{2} \partial_\mu a_i \partial^\mu a_j - \Lambda_n^4 \left[ 1 - \cos \left( N_{ni} \frac{a_i}{f_i} + \delta_n \right) \right], \quad (1.1)$$

where  $K_{ij}$  is the symmetric kinetic mixing matrix,  $f_i$  denotes the decay constant for the  $i$ -th axion  $a_i$ , and summation over repeated indices is understood.  $N$  denotes the instanton charge matrix of the axions, and its component  $N_{ni}$  is the charge of the axion  $a_i$  under the instanton associated to the energy scale  $\Lambda_n$ . We redefine the basis in which  $\frac{a_i}{f_i}$  is  $2\pi$  periodic, i.e.  $\frac{a_i}{f_i} = \frac{a_i}{f_i} + 2\pi$ , so the charges  $N_{ni}$  in eq. (1.1) are all integers.

Like in the case of the field theory axion, the potential in eq. (1.1) may lead to the formation of domain walls (DWs), whose stability depends on the instanton charges  $N_{ni}$ . In the context of field theory, the analogous question of the stability of DWs has been considered for the QCD axion [30–33] and for the case of DWs of other scalar or pseudoscalar fields [34–38]. In the case of the QCD axion, if the PQ phase transition occurs after inflation [30, 39–42], a network of global strings is generated. The strings evolve in the scaling regime until the QCD phase transition, which generates a potential for the axion similar to eq. (1.1) with just one axion ( $i = j = 1$ ) and with instanton charge  $N_{\text{DW}}$ .

At this point, DWs appear and attach to the strings at the location of the maxima of the potential. If  $N_{\text{DW}} > 1$ , the axion potential has multiple minima and the hybrid network of strings and DWs is stable. A familiar example is the DFSZ axion model [43, 44], with  $N_{\text{DW}} = 2N_g$ , where  $N_g$  is the number of generations of fermions that couple to the two Higgs doublets in the model. Nevertheless, the long term survival of the DWs is in severe tension with the observed radiation dominated universe at the time of Big Bang Nucleosynthesis (BBN) [45]. This is the infamous domain wall problem [31] that is due to the fact that the energy density in DWs redshifts more slowly than either matter or radiation. Therefore, a DW network surviving long enough will eventually come to dominate the energy density of the universe [30]. The universe would then enter a regime of accelerated expansion that contradicts the observed cosmology [40].

String theory axions are not associated to a PQ phase transitions, and the formation of topological defects through the Kibble-Zurek mechanism [34, 46] does not take place. On the other hand, in string theory a network of fundamental cosmic strings [47] can be generated by different avenues, such as D-brane annihilation [24, 25, 27]. The evolution of the resulting

axion string network has been considered in [48, 49], the generation of associated DWs has received little attention so far. Consider the case when the strings in the network source the axion flavor state  $a_1$ . Due to the potential in eq. (1.1) we expect the formation of DWs. In this case, the stability of the string domain wall network is dictated by the charge  $N_{11}$ . In particular, for  $N_{11} = 1$  the network is unstable and quickly decays, but if  $N_{11} > 1$ , the potential allows for multiple degenerate minima and the network would be stable. In the absence of good priors for the instanton charges, it is usually assumed that  $N_{ij}$  are arbitrary integers distributed over a large range [50]. We are, thus, led to conclude that a stable DW network is a natural possibility in string theory axion models.

To address the domain wall problem, a mechanism that renders the defect network unstable is required. In the case of field theory axions, it is common to introduce a bias term in the potential, which breaks the PQ symmetry and removes the degeneracy between different vacua [30, 51]. The bias potential can be generated in UV completions, since the PQ symmetry is expected to be violated by Planck suppressed operators [52, 53]. As we discuss below, a bias term that leads to the eventual annihilation of the network naturally appears for string theory axions.

The eventual annihilation of the domain walls and the strings has many interesting consequences, like the production of a stochastic gravitational wave background (SGWB) [36, 37, 54–59] that can be observed with existing [60–62] and upcoming gravitational wave experiments [63–72], or the formation of primordial black holes [73–76]. It can also produce mildly boosted axions, which can contribute to the observed dark matter density in the universe [32, 33, 77, 78]. Axion dark matter has been historically explored in the context of QCD axions. However, axion-like-particles which are not necessarily connected to the strong CP problem are also viable dark matter candidates. For string theory axions, we will find that the annihilation of DWs can produce more than one type of axion dark matter. This provides a complementary observable in addition to the stochastic gravitational wave background.

This paper is organized as follows. We delineate the conditions for the formation of a string-DW network for string theory axions and its stability in Section 2; the evolution and subsequent decay of the DWs are discussed in Section 3. The phenomenological consequences of the annihilation of the defect network are explored in Section 4, and we conclude in Section 5.

## 2 Domain walls of string theory axions

As mentioned above, in extra dimensional UV completions there is no symmetry-breaking PQ phase transition that can seed a network of cosmic strings by the Kibble-Zurek mechanism<sup>1</sup>. Instead, it is generically expected that cosmic strings grow around fundamental strings that can form at the end of D-brane inflation [24, 80–82]. A non-zero field strength remains in the core of the string that can magnetically source the axion (see [49] for examples of this

---

<sup>1</sup>In [79] a scenario in which strings are created in a phase transition associated to the compactification of a warped dimension is discussed. The transition, however, is first order and not associated to a PQ symmetry.

scenario and potential caveats). The axion field configuration surrounding an axion string can naturally form domain walls. The (in)stability of such string domain wall network depends on the details of the axion potential in eq. (1.1). If the axion potential has a single minimum, the domain walls decay shortly after formation. Indeed, since in this case each string is connected to one domain wall, the tension caused by the domain walls pulls the strings together and they quickly annihilate. On the other hand, if the axion potential has multiple minima, each string is attached to more than one domain wall, each pulling the string in different directions. In this case, the network of domain walls is stable. For string theoretic axions, the potential in eq. (1.1) arises from string theory instantons [28]. In this case, the number of minima in axion field space is determined by the instanton charges of that axion. In the absence of a specific prediction for the instanton charges, we can take them to be random integers (in the normalized basis where axions are  $2\pi$  periodic) [50]. Since the magnitude of the charges can naturally be larger than one, the formation of a stable string-domain wall network is a natural possibility.

In particular, let us assume that the strings source the axion flavor state  $a_1$ . The instanton potential naturally couples multiple axions, but for the sake of simplicity, we specialize to the case of two axions,  $a_1$  and  $a_2$ . Among these,  $a_1$  is magnetically sourced by the string. The potential generated by the instanton associated with the largest scale  $\Lambda$  is:

$$V(a_1, a_2) = \Lambda^4 \left[ 1 - \cos \left( N_1 \frac{a_1}{f_1} + N_2 \frac{a_2}{f_2} \right) \right], \quad (2.1)$$

where we have removed an overall phase through a redefinition of the fields. Here,  $N_1$  and  $N_2$  denote the charges of axions  $a_1$  and  $a_2$  respectively. Since the string only sources  $a_1$ , the stability of the string domain wall network is dictated by the charge  $N_1$  and the domain wall number is  $N_{\text{DW}} = N_1$ . In particular, if  $N_1 \neq 1$ , the string domain wall network will be stable, the network reaches the scaling regime [83, 84] and quickly dominates the energy density of the universe. Such a phase in the cosmic history is completely excluded if it occurs close to or after BBN. Although the cosmic history before BBN is less constrained, a domain wall dominated epoch would cause an inflationary expansion of the universe [85] which is difficult to reconcile with the observed cosmology. Either way, the string domain wall network needs to decay eventually. This decay can occur if the multiple minima are not completely degenerate. The energy bias then causes a pressure on different sides of the DWs that leads to their annihilation. For concreteness, we assume that a different instanton generated potential lifts the degeneracy:

$$V_b(a_1) = \frac{\Lambda_b^4}{2} \left[ 1 - \cos \left( N_b \frac{a_1}{f_1} \right) \right] \quad (2.2)$$

where  $\Lambda_b \ll \Lambda$  denotes the scale of the instanton that is responsible for the bias potential, and  $N_b$  the charge of the axion  $a_1$  under the same instanton. We elaborate on the general condition for an instanton generated potential to act as a bias potential in Appendix A. As a simple example, we assume  $N_2 = 1$  and  $N_b = 1$ . This particular choice of charges removes

the degeneracy between multiple minima and leads to the collapse of the network. We also assume the all the string instanton generated potentials are independent of the temperature. It should be noted that, since the energy density of the DWs and other relevant quantities depend linearly on  $N_{\text{DW}}$ , a different choice of the charges would change the numerical details of the phenomenological signatures by an  $\mathcal{O}(1)$  factor.

### 3 Evolution and decay of the string-domain wall network

The thickness  $\delta$  of the domain walls is governed by the mass of  $a_1$ , which is generated by the leading potential  $V$ :

$$\delta^{-1} = \frac{N_1 \Lambda^2}{f_1}. \quad (3.1)$$

The domain walls are effectively “produced” when the horizon size becomes smaller than the thickness of the domain walls,  $H \sim \delta^{-1}$ . At this time, the energy density of the network is dominated by the strings. In the case of field theory axions, the energy density of the string component of the network in the scaling regime [32, 86–89] is given by:

$$\rho_s(t) = \xi \frac{\mu}{t^2}, \quad (3.2)$$

where  $\xi$  is an  $\mathcal{O}(1)$  number,  $\mu$  is the tension in the strings and  $t$  is time. String theory axion strings are qualitatively different from field theory axion strings [49, 90–94]. The structure of the strings depends on the details of the compactification of the extra dimensions, but if warping is not present, the string tension is given by [49]:

$$\mu = \kappa f_1 M_{\text{Pl}}, \quad (3.3)$$

where  $\kappa$  is an  $\mathcal{O}(1)$  number and  $M_{\text{Pl}} = \frac{1}{\sqrt{8\pi G}}$  denotes the reduced Planck mass. This is in contrast with field theory axion strings<sup>2</sup>, which have a parametrically lower tension  $\mu \propto f_1^2$ .

The total energy density in the string theory axion strings is determined by the large number of subhorizon-size string loops. The differential number density of string loops of length  $l$  per unit volume is given by  $n(l, t)$ , so that the total number of strings in a unit volume is  $n(t) = \int n(l, t) dl$ . The simulations differ widely on the size and number density of loops [95–97], and for concreteness, we use the prescription in [49, 95]. The differential number density in the scaling regime is:

$$n(l, t) \approx \frac{\alpha t^{-4}}{\left(\frac{l}{t} + r_G G \mu\right)^{5/2}}, \quad (3.4)$$

where  $\alpha \approx 0.18$  and  $r_G \approx \mathcal{O}(50)$  are model dependent constants [95, 98–100], and  $G$  is the gravitational constant. The expected string length  $\langle l(t) \rangle$  is related to the size of the horizon

---

<sup>2</sup>If warped extra dimensions are involved, like in the scenario presented in [79], the tension could be similar to that of field theory axions.

by:

$$\langle l(t) \rangle \approx H^{-1} \frac{f_1}{M_{\text{Pl}}}. \quad (3.5)$$

We, thus, find that the total energy density in the strings is:

$$\rho_s(t) \approx \mu \langle l(t) \rangle \langle n(t) \rangle \approx \frac{\mu}{t^2} \sqrt{\frac{M_{\text{Pl}}}{f_1}}. \quad (3.6)$$

This is parametrically larger than the energy density of field theory axion strings given in eq. 3.2, which has a number of important phenomenological consequences. The contribution of the strings to the total energy density of the string-domain wall network remains important until much later compared to the standard field theory PQ string. Even more importantly, the GW signal and the amount of axionic DM produced by the strings are much larger.

As for the domain walls, their energy density is negligible compared to the strings immediately after they enter the horizon. For a stable string-domain wall network, the walls themselves quickly reach a scaling regime [101]. As long as the DWs do not dominate the energy density of the universe, their energy density in the scaling regime behaves as:

$$\rho_{\text{dw}}(t) = \mathcal{A} \frac{\sigma}{t}, \quad (3.7)$$

where the so-called ‘‘area parameter’’ is roughly given by  $\mathcal{A} = (0.8 \pm 0.1) N_{\text{DW}}$ , with  $N_{\text{DW}} = N_1$  in our case, and the surface mass density of the domain walls is  $\sigma = 8 f_1 \Lambda^2$  [32].

Since the energy density of the strings redshifts faster than that of the domain walls, after a time  $t_* \sim \frac{M_{\text{Pl}}}{\Lambda^2} \sqrt{\frac{M_{\text{Pl}}}{f_1}}$ , the strings become subdominant. The temperature  $T_* \equiv T(t_*)$  of the universe at this time is:

$$T_* \simeq \Lambda \left( \frac{f_1}{M_{\text{Pl}}} \right)^{\frac{1}{4}} \left( \frac{45}{2\pi^2 g_*} \right)^{\frac{1}{4}} \quad (3.8)$$

where  $g_* \equiv g_*(T_*)$  is the effective number of degrees of freedom, and we have neglected factors of order unity like  $\mathcal{A}$  in this expression for simplicity.

From this point onward, the domain walls dominate the energy density of the universe unless they decay. The eventual demise of the domain walls is brought about by the bias potential, which produces a difference in the potential energy between two successive local minima:

$$\Delta V \approx \Lambda_b^4 \sin^2 \left( \frac{\pi N_b}{N_1} \right) = \Lambda_b^4 \quad (3.9)$$

where in the last equality we have used the values  $N_1 = 2$  and  $N_b = 1$ . The difference in potential energy acts as a pressure against the domain walls and accelerates them towards the true vacuum. When the pressure force roughly equals the surface tension of the walls,

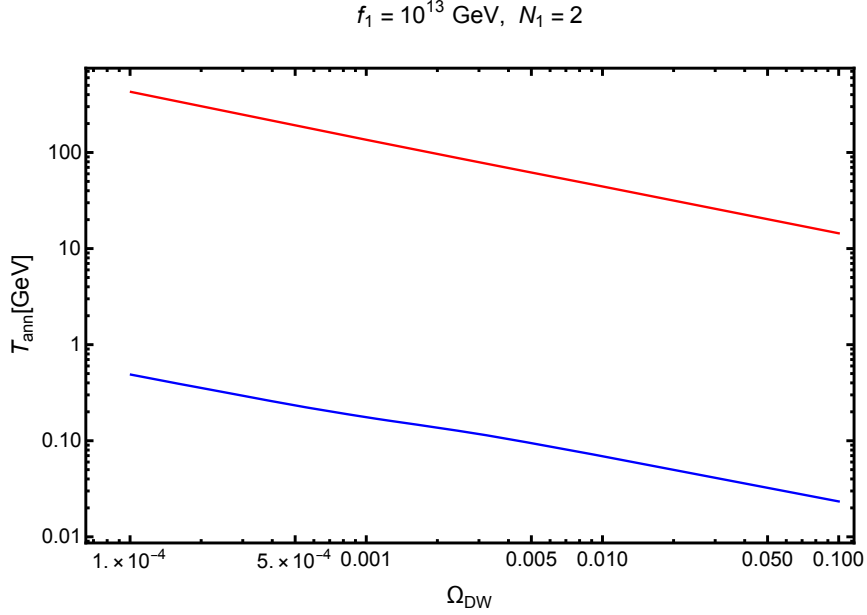


**Figure 1.** The annihilation temperature of the domain walls as a function of the fractional energy density of the domain walls assuming a radiation dominated universe. The red (blue) denotes  $\Lambda = 1 \text{ TeV}$  ( $\Lambda = 1 \text{ GeV}$ ). We see that for natural values of the parameters  $\Lambda$  and  $f$ , the annihilation can happen during electroweak phase transition or at the time of the QCD phase transition.

the domain walls decay. This occurs at the annihilation time:

$$t_{\text{ann}} = C_{\text{ann}} \frac{\mathcal{A}\sigma}{\Delta V} \approx C_{\text{ann}} \frac{8\mathcal{A}f_1\Lambda^2}{\Lambda_b^4}, \quad (3.10)$$

where the proportionality constant  $C_{\text{ann}}$  can be obtained from numerical simulations [32]. In the case of domain walls associated to a  $Z_N$  symmetry [56],  $C_{\text{ann}} \approx 10 - 20$ , independent of the domain wall number. Following [56], we take  $C_{\text{ann}} = 18$  as a benchmark value for the remainder of the paper.

Assuming that the universe is radiation dominated throughout the evolution of the string-domain wall network, we can estimate the temperature of the thermal plasma at the time of annihilation:

$$T_{\text{ann}} \equiv T(t_{\text{ann}}) \approx \frac{\Lambda_b^2}{\Lambda} \left( \frac{M_{\text{Pl}}}{f_1} \right)^{\frac{1}{4}}, \quad (3.11)$$

where we have again ignored  $\mathcal{O}(1)$  factors for clarity. The fractional energy density of the domain walls at the time of annihilation is given by:

$$\Omega_{\text{DW}}(t_{\text{ann}}) = \frac{4 \cdot 8^2}{3} \mathcal{A}^2 C_{\text{ann}} \frac{f_1^2 \Lambda^4}{\Lambda_b^4 M_{\text{Pl}}^2}, \quad (3.12)$$

where  $\Omega_{\text{DW}} = \frac{\rho_{\text{DW}}}{\rho_c}$  is the ratio of the DW energy density to the critical energy density.



For a string theory axion model with a given scale  $\Lambda$  in eq. (2.1), we expect that decreasing the magnitude of the bias potential will push the annihilation of the network to lower temperatures with the DWs attaining a larger energy density. This is borne out in fig. 1, which shows that for reasonable values of the parameters the annihilation can take place at the time of the QCD phase transition, but it could also occur earlier in the evolution of the universe, e.g. during the electroweak phase transition.

### 3.1 Size of the bias term

A domain wall dominated era produces a period of late inflationary expansion, which is extremely difficult to make it compatible with the observed cosmology [85]. The size of the bias potential to avoid a domain wall dominated era can be calculated as follows. As usual, we consider the domain wall evolution in a radiation dominated era, and we defer the discussion of the case of an early matter dominated era (EMD) to app. C. The Hubble parameter at the time of annihilation is given by

$$H_{\text{ann}} = \frac{1}{2} \frac{\Delta V}{C_{\text{ann}} \mathcal{A} \sigma}. \quad (3.13)$$

Demanding that at the time of annihilation, the total energy of the universe is larger than the energy density in the domain walls, i.e.  $\rho_{\text{tot}} > \rho_{\text{DW}}$ , we obtain the constraint:

$$V_b \geq \frac{32\pi}{3} \mathcal{A}^2 C_{\text{ann}} \sigma^2 G \implies \Lambda_b \geq \left( \frac{4\pi}{3} \mathcal{A}^2 C_{\text{ann}} \right)^{\frac{1}{4}} \Lambda \sqrt{\frac{8f_1}{M_{\text{Pl}}}}. \quad (3.14)$$

In addition to producing a pressure force on the network, the presence of the bias potential alters the probability of the axion field choosing the different vacua (which are no longer degenerate). This unequal population of the different vacua in turn biases the domain walls and can also cause the network to decay [33, 35, 102]. But, as shown in app. B, the timescale of annihilation due to this effect is much larger than the timescale corresponding to the pressure force.

On the other hand, a large bias potential can cause the collapse of the string domain-wall network to take place much earlier. In particular, if the bias potential is sufficiently large, the domain wall annihilation time given in eq. 3.10 can occur before  $t_*$ . In that case, the strings dominate the energy density of the network at the time of annihilation. This is avoided if the bias potential remains below:

$$\Lambda_b \leq \Lambda \left( \frac{f_1}{M_{\text{Pl}}} \right)^{\frac{3}{8}}. \quad (3.15)$$

## 4 Phenomenological signatures

As soon as the condition for the decay of the domain walls is met, the network quickly annihilates at the time given in eq. 3.10. More specifically, the fraction of the original network

that survives at time  $t > t_{\text{ann}}$  can be approximated as:

$$f_{\text{DW}} \sim \exp \left[ - \left( \frac{t}{t_{\text{ann}}} \right)^\alpha \right]. \quad (4.1)$$

Although the small number of surviving domain walls makes it challenging to properly estimate this probability, numerical simulations suggest  $\alpha = 3/2$  [103]. This small fraction of late collapsing walls can contribute significantly to the production of primordial black holes [74]. We will not further discuss this interesting signature in quantitative detail given the uncertainties involved [76]. In the following, we focus instead on the generation of gravitational waves and the production of axion dark matter, which mainly take place within one Hubble time of  $t_{\text{ann}}$ .

## 4.1 Production of Gravitational waves

Gravitational waves provide a handle to high energy phenomena in the early universe. As we show below and summarize in fig. 3, the different contributions to the SGWB from the DWs and from the strings generate a unique spectral shape that could allow present and forthcoming experiments to unveil string theory axions.

### 4.1.1 Gravitational waves from domain walls

The production of gravitational waves from the decay of domain walls depends on whether they decay during a radiation dominated epoch or during the more exotic possibility of an early matter dominated epoch. We describe here the former scenario, and we relegate the study of the EMD case to app. C. In appendix E, we show that the axions produced from the annihilation of strings in the scaling regime can not lead to a matter dominated era until the collapse of the whole network. Hence, our assumption that network evolves and collapses in the radiation dominated era is self consistent.

The power radiated in GWs from the annihilation of domain walls can be estimated from the leading quadrupole approximation [104]:

$$P \sim G \ddot{Q}_{ij} \ddot{Q}_{ij}. \quad (4.2)$$

The quadrupole moment of a domain wall can be estimated as  $Q \sim M_{\text{DW}} L(t)^2$ , where  $M_{\text{DW}} \sim \sigma L(t)^2$  is the mass of the wall and  $L(t)$  is its curvature radius, which is  $\propto t$  in the scaling regime. Putting these expressions in eq. (4.2), we get  $P \sim G \sigma^2 t^2$ . The energy density emitted in GWs is:

$$\rho_{\text{gw}} \sim E_{\text{gw}}/t^3 \sim G A^2 \sigma^2. \quad (4.3)$$

The power spectrum of the GWs from DW annihilation is:

$$\Omega_{\text{gw}}(k, t) = \frac{1}{\rho_c(t)} \frac{d\rho_{\text{gw}}(k, t)}{d \log k}. \quad (4.4)$$

The spectrum has a peak in wavenumber corresponding to the annihilation timescale  $k_{\text{peak}}(t_{\text{ann}}) \sim H(t_{\text{ann}})$ . The amplitude of the spectrum is given by:

$$\left(\frac{d\rho_{\text{gw}}}{d \log k}\right)_{\text{peak}} = \epsilon_{\text{gw}} G \mathcal{A}^2 \sigma^2, \quad (4.5)$$

where  $\epsilon_{\text{gw}}$  is an  $\mathcal{O}(1)$  proportionality factor that can be inferred from numerical simulations [32]. For example,  $\epsilon_{\text{gw}} = 5 - 10$  in the case of domain walls associated to a complex scalar with a  $U(1)$  symmetry broken to a  $Z_N$  [32]. However, it should be noted that there are significant uncertainties in  $\epsilon_{\text{gw}}$ . For instance, as found in dedicated numerical simulations of the production of GWs in a radiation dominated universe [58, 103], the domain walls “effectively” decay at  $t \approx 3t_{\text{ann}}$ , which increases the amplitude of the GW power spectrum by a factor of  $\sim 10$ . Nevertheless, to obtain a conservative estimate of the amplitude of the GW background, we will assume that the network annihilates at  $t \approx t_{\text{ann}}$ .

The frequency scale corresponding to the highest power,  $f_{\text{peak}}$ , is simply related to the Hubble parameter during annihilation:

$$f_{\text{peak}} = H(t_{\text{ann}}) \frac{R(t_{\text{ann}})}{R(t_0)} = H(t_{\text{ann}}) \frac{T_0}{T_{\text{ann}}}, \quad (4.6)$$

where  $R(t)$  denotes the scale factor at time  $t$ , and the subscript 0 refers to the present epoch. In the last equality we have assumed a radiation dominated universe. Since  $H(t_{\text{ann}}) \propto T_{\text{ann}}^2$ , the spectrum peaks at higher frequencies as the annihilation happens earlier. For lower frequencies,  $f < f_{\text{peak}}$ , the spectrum has the usual causal tail [105, 106]  $\Omega_{\text{gw}} \propto f^3$ ; and the power decays as  $\Omega_{\text{gw}} \propto f^{-1}$  for higher frequencies,  $f_{\delta} > f > f_{\text{peak}}$ , as confirmed by numerical simulations [32]. The frequency  $f_{\delta}$  is another important scale in the spectrum, and it corresponds to the width of the domain walls:

$$f_{\delta} = \delta^{-1} \frac{R(t_{\text{ann}})}{R(t_0)} = \delta^{-1} \frac{T_{\text{ann}}}{T_0}. \quad (4.7)$$

Since this is the smallest scale in the network, the power at scales below this one is extremely suppressed, as noted in the simulations [32]. The precise scaling of the power spectrum beyond this frequency is difficult to obtain from numerical simulations, although there are some hints that the power increases as the number of domain walls,  $N_{DW}$ , increases. The GW energy density at the time of annihilation is given by:

$$\Omega_{\text{gw}}(t_{\text{ann}})_{\text{peak}} = \frac{1}{\rho_c(t_{\text{ann}})} \left(\frac{d\rho_{\text{gw}}(t_{\text{ann}})}{d \log k}\right)_{\text{peak}} = \frac{8\pi\epsilon_{\text{gw}} G^2 \mathcal{A}^2 \sigma^2}{3H^2(t_{\text{ann}})}. \quad (4.8)$$

As noted above, the majority of the domain walls decay shortly after  $t_{\text{ann}}$ . In the limit of

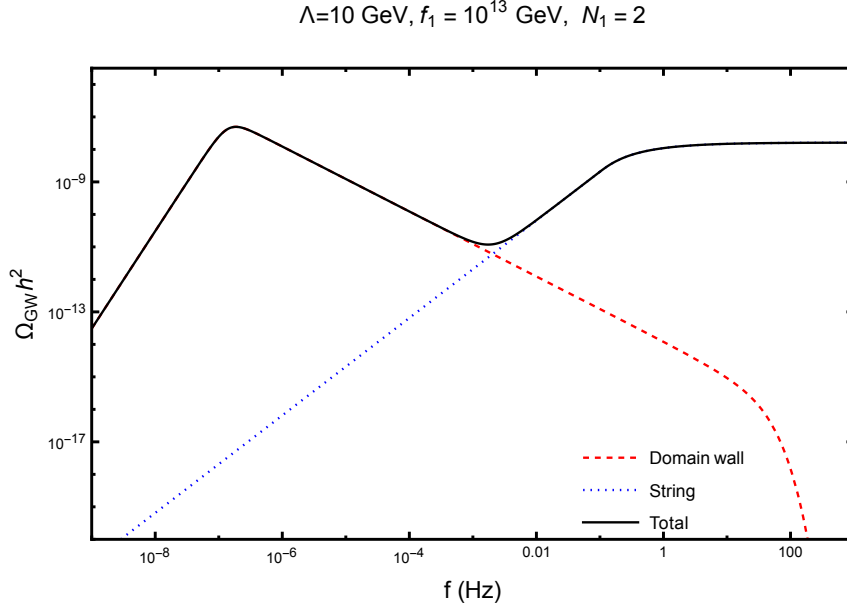


**Figure 2.** The red-dashed curve shows the gravitational wave spectrum produced by the domain walls for  $\Lambda = 10 \text{ GeV}$ ,  $f_1 = 10^{13} \text{ GeV}$ ,  $N_1 = 2$  and  $\rho_{\text{dw}}(t_{\text{ann}}) = 10^{-2} \rho_{\text{tot}}(t_{\text{ann}})$ . The blue-dotted line shows the spectrum produced by the string network, and the combined spectrum is depicted by the black curve. String theory axion strings produce larger amounts of GWs because of their higher tension. The high energy tail corresponds to the logarithmic divergence in the total GW energy emitted by the strings.

instantaneous decay, the GW power spectrum measured today is given by:

$$\begin{aligned} \Omega_{\text{gw}} h^2(t_0) &= \frac{\rho_{\text{gw}}(t_0) h^2}{\rho_c(t_0)} = \frac{\rho_c(t_{\text{ann}}) h^2}{\rho_c(t_0)} \left( \frac{R(t_{\text{ann}})}{R(t_0)} \right)^4 \Omega_{\text{gw}}(t_{\text{ann}}) \\ &= \Omega_{\text{rad}} h^2 \left( \frac{g_*(T_{\text{ann}})}{g_{*0}} \right) \left( \frac{g_{*s0}}{g_{*s}(T_{\text{ann}})} \right)^{4/3} \Omega_{\text{gw}}(t_{\text{ann}}), \end{aligned} \quad (4.9)$$

where  $g_{*0} = 3.36$  and  $g_{*s0} = 3.91$  are the number of relativistic degrees of freedom for the energy density and the entropy density respectively at the present time; while  $g_*(T_{\text{ann}})$  and  $g_{*s}(T_{\text{ann}})$  are the corresponding values at  $t = t_{\text{ann}}$ . We have used the formulae in [107] to numerically evaluate  $g_*(T)$  and  $g_{*s}(T)$ .

#### 4.1.2 Gravitational waves from strings in the scaling regime

Until now, we have not considered the energy density of the strings in discussing the GW power spectrum. However, depending on the size of the bias potential, the network might annihilate at a time when the strings dominate the net energy density of the network. In particular, when the bias potential is sufficiently large to violate eq. 3.15, the contribution of the strings to the GW power spectrum can no longer be neglected.

The energy density of the strings in the scaling regime redshifts as  $\rho_s \sim \frac{\mu}{t^2} \sqrt{\frac{M_{\text{Pl}}}{f_1}}$ . Con-

servation of energy requires the strings to continuously radiate energy at a rate  $\Gamma \sim d\rho_s / dt$ , where  $\Gamma$  denotes the energy radiated by the string network per unit time per unit volume. The strings emit gravitational waves and axions, but under certain assumptions [49] the respective emission rates are parametrically equal. The energy radiated in GWs per unit time per unit volume from string loops is:

$$\Gamma_{\text{gw}} = \frac{16\alpha r_G \sqrt{8\pi\kappa}}{3r^{3/2}} H^3 \sqrt{f_1 M_{\text{Pl}}^3}, \quad (4.10)$$

where we have used eq. 3.3 for the string tension  $\mu$ ; the constants  $\kappa$ ,  $\alpha$ ,  $r_G$  were defined in sec. 3; and  $r = r_G + r_a \frac{8\pi}{\kappa^2}$  accounts for GW as well as axion emission, with  $r_a \approx \mathcal{O}(10)$  [108, 109] a dimensionless constant.

The GW spectrum is determined by how the total power is distributed among gravitational radiation at different frequencies. The spectrum of gravitational radiation emitted by a single loop of length  $\ell$  depends on the shape of the loop, with a lower cutoff frequency  $\omega_\ell \geq 4\pi/\ell$ . For an ensemble of string loops, the spectrum can be approximated by a power law. Namely, the energy emitted from loops of length  $\ell$  is:

$$\frac{d\dot{E}_{\text{GW}}^\ell}{d\omega} = r_G G \mu^2 \begin{cases} 0 & \omega < \omega_\ell \\ \omega_1^{q-1} \frac{q-1}{\omega^q} & \omega > \omega_\ell. \end{cases} \quad (4.11)$$

The total GW emission per unit time per unit volume averaged over the string network is then:

$$\frac{d\Gamma_{\text{gw}}(t, \omega)}{d\omega} = \int d\ell n(\ell, t) \frac{d\dot{E}_{\text{gw}}^\ell}{d\omega}. \quad (4.12)$$

Finally, the total energy density in GWs at some time  $t$  can be calculated from the emission rate:

$$\frac{d\rho_{\text{gw}}(t, \omega)}{d\omega} = \int_0^t dt' \left( \frac{R(t')}{R(t)} \right)^3 \frac{d\Gamma_{\text{gw}}(t', \omega')}{d\omega'}, \quad (4.13)$$

where  $\omega' = \omega R(t)/R(t')$  accounts for the redshift of the GW frequency. To obtain the gravitational wave energy density emitted by the string network, one needs to numerically evaluate eq. 4.13 for a specific cosmological history. However, under the assumption that the number of radiation-like degrees of freedom remains unchanged throughout the evolution of the strings, it is possible to write the total gravitational wave energy density as:

$$\frac{d\rho_{\text{gw}}(\omega, t)}{d\omega} = \Gamma_{\text{gw}} \frac{x_{\text{UV}}}{5 \cdot 8\pi \cdot H^2} \mathcal{F}(\omega/\omega_0), \quad (4.14)$$

where  $x_{UV} = r_G G\mu$ ,  $\omega_0 = 8\pi H/x_{UV}$ , and we have defined:

$$\mathcal{F}(x) \equiv \begin{cases} \frac{4(q-1)}{2q+1} \sqrt{x}, & \text{if } x \leq 1 \\ \frac{1}{2-q} \left[ 3(q-1)x^{-2} - \frac{15}{2q+1}x^{-q} + 5(2-q)x^{-1} \right], & \text{if } x > 1. \end{cases} \quad (4.15)$$

The string network produces gravitational radiation until the annihilation of the network at time  $t_{\text{ann}}$ . Afterwards, the gravitational waves redshift without significant interaction with the matter and radiation. The gravitational wave power spectrum observed today is then:

$$\begin{aligned} h^2 \frac{d\Omega_{\text{gw},0}}{d \log \omega} &\equiv \frac{h^2}{\rho_{c,0}} \frac{d\rho_g(t_0, \omega)}{d \log \omega} \\ &= \frac{h^2}{\rho_{c,0}} \left( \frac{R_{\text{ann}}}{R_0} \right)^4 \frac{d\rho_g(t_{\text{ann}}, \omega R_0/R_{\text{ann}})}{d \log \omega} \\ &= \frac{16\sqrt{2}\pi^5}{2025} \frac{g_{*,\text{ann}} g_{*,s,0}^{4/3}}{g_{*,s,\text{ann}}^{4/3}} \frac{h^2 T_0^4}{H_0^2 M_{\text{Pl}}^2} \left( \frac{r_G \sqrt{\kappa\alpha}}{r^{3/2}} \right) \sqrt{\frac{f_1}{M_{\text{Pl}}}} x \mathcal{F}(x) \Big|_{x=\frac{R_0\omega}{R_{\text{ann}}\omega_{0,\text{ann}}}}. \end{aligned} \quad (4.16)$$

Fig. 2 shows the stochastic gravitational wave background produced by the string network, assuming that the emission is dominated by kinks,  $q = 5/3$  [110]. Interestingly, the total GW spectrum shows the distinctive signature of the low frequency peak from the domain wall decay, as well as the high frequency tail from the strings. Observation of such a singular GW background would be a smoking gun of string theory axion strings. For reasonable values of the parameters, fig. 3 shows how this can be achieved through a combination of low-frequency radio telescope observations that could probe the DW contribution, together with observations at higher frequencies that could map the contribution from strings (e.g. by space-borne LISA or next-generation ground based GW observatories).

## 4.2 Production of axion dark matter

The annihilation of the network produces mildly relativistic axions [32]. The network emits the flavor eigenstate  $a_1$  it couples to, but the abundance of axions in the late universe is dictated by the properties of the mass eigenstates. As noted in [49], kinetic mixing does not alter the abundance of axion mass eigenstates barring some extreme fine-tuned scenarios where the mass mixing is canceled exactly due to kinetic mixing. Therefore, we can ignore kinetic mixing without forgoing any interesting property of the axion mass eigenstates.

The mass matrix for the axion flavor states is given by (using the notation in [49]):

$$\mathcal{L} \supset -\frac{1}{2} \begin{pmatrix} a_1 \\ a_2 \end{pmatrix}^\top \begin{pmatrix} M_{a_1}^2 & M_{a_1 a_2}^2 \\ M_{a_1 a_2}^2 & M_{a_2}^2 \end{pmatrix} \begin{pmatrix} a_1 \\ a_2 \end{pmatrix}, \quad (4.17)$$

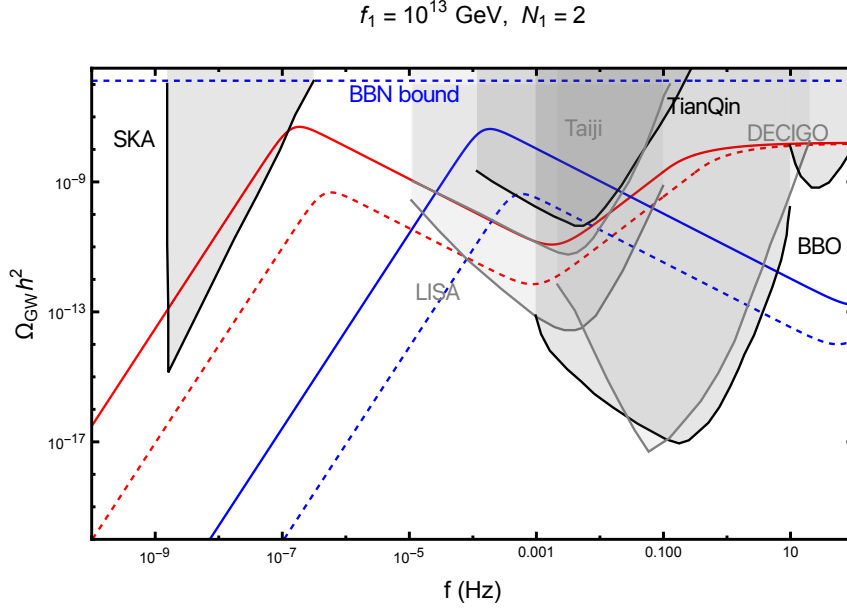


**Figure 3.** The gravitational wave spectrum produced by the collapse of domain walls with instanton scales  $\Lambda = 10$  GeV (red) and  $\Lambda = 10$  TeV (blue). The axion decay constant and the domain wall number are set to  $f_1 = 10^{13}$  GeV and  $N_1 = 2$ . The solid and the dashed lines depict  $\rho_{\text{DW}}(t_{\text{ann}}) = 10^{-2}\rho_{\text{tot}}(t_{\text{ann}})$  and  $\rho_{\text{DW}}(t_{\text{ann}}) = 10^{-3}\rho_{\text{tot}}(t_{\text{ann}})$  respectively.

where the elements of the mass matrix are:

$$\begin{aligned}
 M_{a_1}^2 &= \frac{N_1^2 \Lambda^4 + N_b^2 \Lambda_b^4}{f_1^2}, \\
 M_{a_2}^2 &= \frac{N_2^2 \Lambda^4}{f_2^2}, \\
 M_{a_1 a_2}^2 &= \frac{N_1 N_2 \Lambda^4}{f_1 f_2}.
 \end{aligned} \tag{4.18}$$

The mass eigenstates  $(\phi_2, \phi_1)$  obtained after diagonalizing eq. 4.17 can be written in terms of rotated flavor states  $(a_1, a_2)$  as:

$$\begin{pmatrix} \phi_2 \\ \phi_1 \end{pmatrix} = R(\theta) \begin{pmatrix} a_1 \\ a_2 \end{pmatrix}, \tag{4.19}$$

where

$$R(\theta) = \begin{pmatrix} \cos \theta & \sin \theta \\ -\sin \theta & \cos \theta \end{pmatrix}. \tag{4.20}$$

The rotation angle is:

$$\begin{aligned}
\cos 2\theta &= \frac{M_{a_1}^2 - M_{a_2}^2}{\Delta^2}, \\
\sin 2\theta &= \frac{2M_{a_1 a_2}^2}{\Delta^2}, \\
(\Delta^2)^2 &= (M_{a_1}^2 - M_{a_2}^2)^2 + 4(M_{a_1 a_2}^2)^2.
\end{aligned}
\tag{4.21}$$

And we finally obtain the masses of the mass eigenstates:

$$\begin{aligned}
M_{\varphi_1}^2 &= \frac{1}{2} (M_{a_1}^2 + M_{a_2}^2 - \Delta^2), \\
M_{\varphi_2}^2 &= \frac{1}{2} (M_{a_1}^2 + M_{a_2}^2 + \Delta^2),
\end{aligned}
\tag{4.22}$$

where we have assumed that  $\phi_2$  is the heavier mass eigenstate,  $M_{\phi_2} > M_{\phi_1}$ .

Some important properties of the mass eigenstates are immediately apparent. The constraint that must be satisfied between the instanton scales  $\Lambda$  and  $\Lambda_b$  to prevent domain walls from dominating the energy density of the universe is given by eq. 3.14, which can be schematically cast in the form  $\Lambda_b \sim \Lambda \sqrt{\frac{f_1}{M_{\text{Pl}}}}$ . From eq. (3.12), we deduce that the scale of the bias potential that corresponds to the domain walls having a given fractional energy density is given by  $\Lambda_b \sim \Omega_{DW}(t_{\text{ann}})^{-\frac{1}{4}} \Lambda \sqrt{\frac{f_1}{M_{\text{Pl}}}}$ . Hence, in order for the the domain walls to have any observable effects, we need the instanton scales to be well separated,  $\Lambda \gg \Lambda_b$ . This suggests that the heavier mass eigenstate is predominantly the linear combination of flavor eigenstates that couples to the instanton with the larger scale,  $\phi_2 \sim N_1 a_1 + N_2 \left(\frac{f_1}{f_2}\right) a_2$ .

The axions (mass eigenstates) can decay into both standard model and other axions. Decays into other axions are suppressed in the case of large hierarchies between instanton scales [111], while decays into standard model particles are highly model dependent. In many explicit construction of a particular string model, the coupling of the axions to QCD is natural [13]. The decay to gluons can be readily estimated and is negligible [112] for small masses, but it can be significant for heavier axions. The couplings to fermions are highly model dependent [49], so we will only consider the decay to photons in the following. Depending on the masses of the eigenstates, the overlap between these axions and the QCD axion can be negligible [113], which can suppress the coupling to photons. However, for several explicit string theory constructions this coupling appears to be robust [111]. The coupling of the flavor states to photons can be naturally parameterized by:

$$C_\alpha \equiv 2\pi \frac{g_{a\gamma\gamma} f_a}{\alpha_{\text{EM}}},
\tag{4.23}$$

where  $g_{a\gamma\gamma}$  is the axion coupling to photons and  $\alpha_{\text{EM}}$  is the fine structure constant. It is often a good approximation to assume  $C_\alpha \sim 1$ . The width associated to the decay of a mass



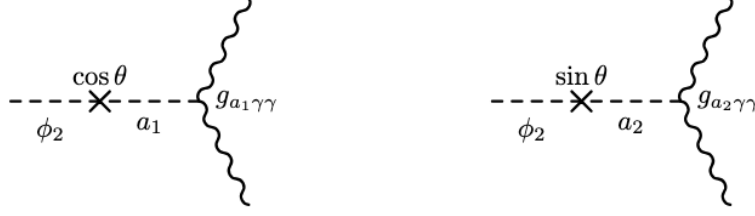


**Figure 4.** The decay of the heavier mass eigenstate  $\phi_2$  to two photons. It can be clearly seen that the total decay width is proportional to the couplings given in eq. 4.25.

eigenstate to two photons is then given by:

$$\Gamma_{\phi_i \rightarrow \gamma\gamma} = \frac{M_{\phi_i}^3 g_{\phi_i \gamma\gamma}^2}{64\pi}, \quad i = 1, 2, \quad (4.24)$$

with the coupling constants:

$$g_{\phi_2 \gamma\gamma}^2 = g_{a_1 \gamma\gamma}^2 \cos^2 \theta + g_{a_2 \gamma\gamma}^2 \sin^2 \theta, \quad g_{\phi_1 \gamma\gamma}^2 = g_{a_1 \gamma\gamma}^2 \sin^2 \theta + g_{a_2 \gamma\gamma}^2 \cos^2 \theta. \quad (4.25)$$

Since the axion decay constants,  $f_a$ , are in general distributed rather narrowly [111], we assume that  $f_1 = f_2 = f$  for concreteness. In this approximation, the coupling to photons is then given by:

$$g_{\phi_i \gamma\gamma} = \frac{\alpha_{\text{EM}}}{2\pi f}. \quad (4.26)$$

In the limit  $\Lambda \gg \Lambda_b$ , we can write down the masses and the mixing angle:

$$\begin{aligned} M_{\phi_1}^2 &= \frac{N_2^2 N_b^2}{(N_1^2 + N_2^2)} \frac{\Lambda_b^4}{f^2}, \\ M_{\phi_2}^2 &= (N_1^2 + N_2^2) \frac{\Lambda^4}{f^2}, \\ \theta &= \frac{1}{2} \sin^{-1} \left( \frac{2N_1 N_2}{N_1^2 + N_2^2} \right). \end{aligned} \quad (4.27)$$

With the canonical coupling to photons given by eq. 4.26, the lifetime of the heavier mass eigenstates turns out to be:

$$\tau_{\phi_2} = \frac{256\pi^3 f^5}{(N_1^2 + N_2^2)^{\frac{3}{2}} \alpha_{\text{EM}}^2 \Lambda^6} = 8.8 \times 10^{20} \text{ s} \left( \frac{f}{10^{10} \text{ GeV}} \right)^5 \left( \frac{10^2 \text{ GeV}}{\Lambda} \right)^6 \quad (4.28)$$

where we have used  $N_1 = 2$  and  $N_2 = 1$ . These are the values that we use through the rest of this section. As can be seen from Fig. 5, for some part of the parameter space the heavier

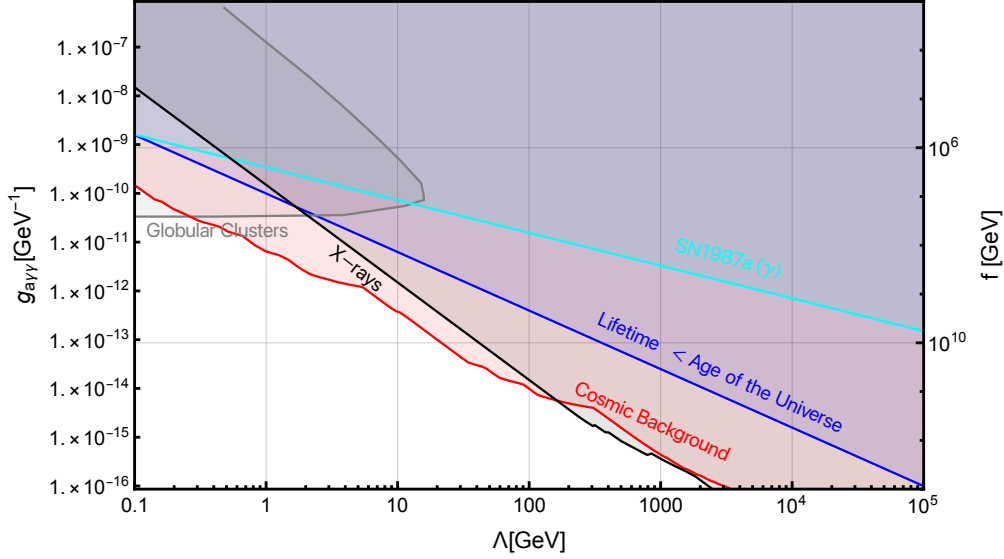


**Figure 5.** Existing astrophysical and cosmological constraints on the heavy mass eigenstate assuming canonical coupling to photons. The bounds displayed are from SN1987a [114–116] (Cyan), from the cosmic microwave background [117] (red), from the  $R$  and  $R_2$  parameters in Globular clusters [118, 119] (gray), and from X-ray observations [120] (black).

mass eigenstate has a lifetime shorter than the age of the universe, so they cannot constitute the dark matter in the universe. On the other hand, the bulk of the currently unconstrained parameter space corresponds to the heavier axion having a lifetime that is much longer than the age of the universe, so it can potentially constitute the dark matter in the universe subject to other constraints from X-rays and CMB, as shown in Fig. 5. However, once we take into account the relic abundance, the viable part of the parameter space is reversed. As we now show, the heavier eigenstate is typically overproduced, which is excluded unless it decays fast enough. If the heavy state is long lived compared to the annihilation time of the DWs, but short lived compared to the time of BBN, then it could dominate the energy density of the universe for a short period of time and then decay, leading to an EMD era.

Let us now, thus, discuss the axion abundances generated by different production mechanisms.

#### 4.2.1 Axions from the collapse of domain walls

Moderately relativistic axions produced from the collapse of the network can serve as the cold dark matter. Let us first, for simplicity, discuss the production from the domain walls, ignoring for the moment the contribution of the strings. In this case, the evolution of the energy density in domain walls  $\rho_{\text{dw}}$ , axions  $\rho_a$ , and gravitational waves  $\rho_{\text{gw}}$  is given by the

coupled differential equations:

$$\frac{d\rho_{\text{dw}}}{dt} = -H\rho_{\text{dw}} - \left. \frac{d\rho_{\text{dw}}}{dt} \right|_{\text{emission}}, \quad (4.29)$$

$$\frac{d\rho_a}{dt} = -3H\rho_a + \frac{d\rho_{\text{dw}\rightarrow a}}{dt}, \quad (4.30)$$

$$\frac{d\rho_{\text{gw}}}{dt} = -4H\rho_{\text{gw}} + \frac{d\rho_{\text{dw}\rightarrow\text{gw}}}{dt}, \quad (4.31)$$

where

$$\left. \frac{d\rho_{\text{dw}}}{dt} \right|_{\text{emission}} = \frac{d\rho_{\text{dw}\rightarrow a}}{dt} + \frac{d\rho_{\text{dw}\rightarrow\text{gw}}}{dt}. \quad (4.32)$$

From eqs. 3.7 and 4.5, we find:

$$\left. \frac{d\rho_{\text{dw}}}{dt} \right|_{\text{emission}} = \mathcal{A} \frac{\sigma_{\text{dw}}}{2t^2}, \quad (4.33)$$

and:

$$\frac{d\rho_{\text{dw}\rightarrow\text{gw}}}{dt} = \frac{2\epsilon_{\text{gw}}G\mathcal{A}^2\sigma_{\text{dw}}^2}{t}. \quad (4.34)$$

The total energy emitted in the form of axions per unit comoving volume is given by:

$$E_a(t) \equiv R^3(t)\rho_a(t) = \int_{t_i}^t dt' R^3(t') \left[ \frac{\mathcal{A}\sigma_{\text{dw}}}{2t'^2} - \frac{2\epsilon_{\text{gw}}G\sigma_{\text{dw}}^2\mathcal{A}^2}{t'} \right], \quad (4.35)$$

where  $t_i$  is the time when the wall begins to radiate axions, which we can assume to be equal to the wall formation time. For  $t \gg t_i$ , the total energy in axions is then found to be:

$$E_a(t) \simeq R^3(t) \left( \mathcal{A} \frac{\sigma_{\text{dw}}}{t} - \frac{4}{3} \epsilon_{\text{gw}} G \sigma_{\text{dw}}^2 \mathcal{A}^2 \right). \quad (4.12)$$

The walls emit axions in the flavor state that they couple to [49], which in our model is  $a_1$ . We can then find the abundance of the different mass eigenstates at late times by projecting the mass eigenstates onto the flavor eigenstate  $a_1$ . More explicitly:

$$E_{\phi_2}(t) = E_a(t) \cos^2 \theta \quad \text{and} \quad E_{\phi_1}(t) = E_a(t) \sin^2 \theta, \quad (4.36)$$

where the mixing angle  $\theta$  was obtained in eq. 4.21. We can relate the total energy emitted in the form of axions to the width of the wall:

$$\frac{E_{\phi_i}(t)}{N_{\phi_i}(t)} = \sqrt{1 + \epsilon_a^2} \left( \frac{1}{\delta} \right), \quad (4.37)$$

where  $\delta = \frac{f_1}{N_1 \Lambda^2}$  is the width of the wall, and  $\epsilon_a$  can be obtained from simulations. The numerical experiments in [32, 77] show that  $\epsilon_a$  has a mild dependence on the domain wall number and, while it increases slightly for large values of the domain wall number, it falls in

the range  $\epsilon_a \approx 1.2 - 1.5$ . Once the domain walls have annihilated, no more axions are being produced. If they are long lived, for times within their lifetime, the number density of axions per comoving volume does not change:

$$n_{\phi_i}(t) = n_{\phi_i}(t_0) \left( \frac{R(t_{\text{ann}})}{R(t_0)} \right)^3. \quad (4.38)$$

The axions emitted by the walls are mildly relativistic at the time of emission [32, 77], and they evolve to contribute to the population of cold axions today. The energy density in the mass eigenstates today is:

$$\rho_{\phi_i}(t) = n_{\phi_i}(t) M_{\phi_i}, \quad (4.39)$$

which corresponds to a fractional energy density:

$$\left( \frac{\Omega_{\phi_2, \text{DW}}(t_0)}{\Omega_{\phi_1, \text{DW}}(t_0)} \right) = \frac{1}{\rho_c(t_0)} \frac{\delta}{\sqrt{1 + \epsilon_a^2}} \left( \mathcal{A} \frac{\sigma_{\text{dw}}}{t_{\text{ann}}} - \frac{4}{3} \epsilon_{\text{gw}} G \sigma_{\text{dw}}^2 \mathcal{A}^2 \right) \left( \frac{R(t_{\text{ann}})}{R(t_0)} \right)^3 \times \left( \frac{\cos^2 \theta M_{\phi_2}}{\sin^2 \theta M_{\phi_1}} \right), \quad (4.40)$$

where  $\frac{R(t_{\text{ann}})}{R(t_0)} = \left( \frac{g_{*s,0}}{g_{*,s,\text{ann}}} \right)^{1/3} \frac{T_0}{T_{\text{ann}}}$ , and  $H_0 = 1.4 \times 10^{-33} \text{eV}$ ,  $T_0 = 2.4 \times 10^{-4} \text{eV}$  are the Hubble constant and the photon temperature today. Nominally,  $\Omega_{\phi_i, \text{dw}}$  in eq. 4.40 can become negative if the network annihilation happens sufficiently late,  $\Omega_{\text{dw}}(t_{\text{ann}}) > \frac{8\pi}{\epsilon_{\text{gw}}} > 1$ . In this case, eq. 4.40 breaks down, since the backreaction of the gravitational waves emitted by the domain walls becomes important [32]. This regime is naturally avoided as long as the domain walls do not dominate the energy density of the universe. Indeed, when  $\Omega_{\text{dw}}(t_{\text{ann}}) \ll 1$ , it is a good approximation to ignore the negative contribution of the gravitational wave emission. In that case, using eq. 4.27, we find:

$$\Omega_{\phi_2, \text{dw}}(t_0) \approx c_1 \left( \frac{f}{M_{\text{Pl}}} \right)^{3/2} \frac{\Lambda^3 T_0^3 \cos^2 \theta}{\Lambda_b^2 \rho_{c,0}} = 7.9 \left( \frac{\Lambda}{10^2 \text{GeV}} \right)^3 \left( \frac{1 \text{GeV}}{\Lambda_b} \right)^2 \left( \frac{f}{10^{10} \text{GeV}} \right)^{\frac{3}{2}}, \quad (4.41)$$

$$\Omega_{\phi_1, \text{dw}}(t_0) \approx c_2 \left( \frac{f}{M_{\text{Pl}}} \right)^{3/2} \frac{\Lambda T_0^3 \sin^2 \theta}{\rho_{c,0}} = 3.9 \times 10^{-5} \left( \frac{\Lambda}{10^2 \text{GeV}} \right) \left( \frac{f}{10^{10} \text{GeV}} \right)^{\frac{3}{2}}, \quad (4.42)$$

where  $c_1 = 12 \left( \frac{g_{*s,0}}{g_{*,s}(T_{\text{ann}})} \right) \left( \frac{(N_1^2 + N_2^2) \mathcal{A}^3 C_{\text{ann}}}{N_1^2 g_*(T_{\text{ann}})^{3/2} (1 + \epsilon_a^2)} \right)^{\frac{1}{2}}$  and  $c_2 = c_1 \left( \frac{N_2^2 N_b^2}{(N_1^2 + N_2^2)} \right)^{\frac{1}{2}}$  are dimensionless quantities. It should be noted that  $c_1$  and  $c_2$  have a mild dependence on  $\Lambda$ ,  $\Lambda_b$  and  $f$ , which we have neglected in the second part of eqs. 4.41 and 4.42.

### 4.2.2 Axions from the misalignment mechanism

In addition to the dark matter axions sourced by the domain wall network, the total axion dark matter abundance also includes a contribution from the misalignment mechanism. Barring the presence of a large initial kinetic energy of the axion field, the zero mode remains frozen

until the axion field evolution becomes underdamped,

$$M_{\phi_i} \simeq 3H(t_{\text{osc},i}) \quad (4.43)$$

where  $t_{\text{osc},i}$  is the time when the  $i$ th mass eigenstate begins to oscillate. Since the instanton potential is time independent, the masses of the mass eigenstates  $M_{\phi_i}$  are also time independent, unlike the case of the QCD axion. The total energy density in each mass eigenstate from misalignment is then given by:

$$\rho_{\phi_i,\text{mis}}(t_0) = \frac{1}{2} M_{\phi_i}^2 \langle \theta_{i,\text{mis}}^2 \rangle f_{\phi_i}^2 \left( \frac{R(t_{\text{osc}})}{R(t_0)} \right)^3 \quad (4.44)$$

where  $\theta_i = \frac{a_i}{f_i}$ . We are neglecting possible anharmonic effects in the axion field evolution that could be important if  $\langle \theta_{i,\text{mis}} \rangle$  is close to  $\pi$  [121–126]. The initial misalignments of the mass eigenstates are:

$$\langle \theta_{2,\text{mis}}^2 \rangle f_{\phi_2}^2 \approx \frac{\pi^2}{3} (f_1 \cos \theta + f_2 \sin \theta)^2, \quad \langle \theta_{1,\text{mis}}^2 \rangle f_{\phi_1}^2 \approx \frac{\pi^2}{3} (f_1 \sin \theta + f_2 \cos \theta)^2, \quad (4.45)$$

where we have approximated the initial values  $a_i/f_i$  to be uniformly distributed. We further elaborate on this aspect in App. D. Taking the benchmark values  $f_1 = f_2 = f$ , we find the fractional axion energy density from misalignment:

$$\Omega_{\phi_2,\text{mis}}(t_0) \approx c_3 \left( \frac{f}{M_{\text{Pl}}} \right)^{3/2} \frac{T_0^3 \Lambda}{\rho_{c,0}} = 0.42 \left( \frac{\Lambda}{10^2 \text{GeV}} \right) \left( \frac{f}{10^{10} \text{GeV}} \right)^{\frac{3}{2}} \quad (4.46)$$

$$\Omega_{\phi_1,\text{mis}}(t_0) \approx c_4 \left( \frac{f}{M_{\text{Pl}}} \right)^{3/2} \frac{T_0^3 \Lambda_b}{\rho_{c,0}} = 1.9 \times 10^{-4} \left( \frac{\Lambda_b}{1 \text{GeV}} \right) \left( \frac{f}{10^{10} \text{GeV}} \right)^{\frac{3}{2}}, \quad (4.47)$$

where  $c_3 = 1.6 \left( \frac{g_{*s,0}}{g_{*s,2}} \right) \frac{(N_1 + N_2)^2 g_{*2}^{3/4}}{(N_1^2 + N_2^2)^{3/4}}$  and  $c_4 = 1.6 \left( \frac{g_{*s,0}}{g_{*s,1}} \right) \frac{(N_1 + N_2)^2 g_{*1}^{3/4}}{(N_1^2 + N_2^2)^{3/4}} (N_2^2 N_b^2)^{1/4}$  are dimensionless coefficients, and  $g_{*,i} = g_*|_{M_{\phi_i}=3H}$  is evaluated at the time when the mass eigenstates start to oscillate. Once more, we have neglected the mild dependence of  $c_3$  and  $c_4$  on  $\Lambda, \Lambda_b, f$  that enters through  $g_{*,i}$ .

### 4.2.3 Axion emission from strings in the scaling regime

Most of the numerical studies of axion emission from field theory strings are performed in the context of  $N_{\text{dw}} = 1$  models with unstable domain walls [30, 39, 41, 127–138]. In this case, the results of the simulations are consistent with the assumption that the network of strings emits relativistic axions with a spectrum  $dE_a/d\omega \sim 1/\omega$ . On the other hand, in the case of a stable string domain wall network in models with  $N_{\text{dw}} > 1$ , existing numerical simulations generally introduce a bias potential that causes the network to decay at a time when the energy of the strings is subdominant compared to that of the domain walls [32]. As a result, the bulk of the axion emission is constituted by the mildly relativistic axions produced by the

domain walls, while the strings in the scaling regime merely contribute a residual long tail to the spectrum.

The axion emission from strings in a string theory axiverse scenario with flat extra dimensions was studied in [49]. In this case, the rate of energy emission in mass eigenstates is related to the energy emitted in flavor states by:

$$\frac{dE_{\phi_1}}{dt} = \frac{dE_{a_1}}{dt} \sin^2 \theta \quad \frac{dE_{\phi_2}}{dt} = \frac{dE_{a_1}}{dt} \cos^2 \theta \quad (4.48)$$

where  $E_{a_1}$  and  $E_{\phi_i}$  are the energy emitted in the flavor state  $a_1$  and in the mass eigenstate  $\phi_i$  respectively; and  $\theta$  is the mixing angle defined in eq. 4.21. The total power emitted per unit volume is found by adding the contributions of loops of different sizes present in the network:

$$\Gamma_{\phi_i}(t) = \int \frac{dE_{\phi_i}}{dt} n(\ell, t) d\ell. \quad (4.49)$$

Assuming an axion spectrum of the form  $\frac{d\dot{E}_a}{d\omega} \sim 1/\omega$ , we obtain the number density of axions emitted until time  $t$ :

$$n_{\phi_2}(t) \approx \frac{4}{3} \sqrt{\frac{2}{\pi}} \frac{r_a \alpha}{\sqrt{r\kappa}} H f \frac{\sqrt{f M_{\text{Pl}}}}{\log\left(\frac{M_{\text{Pl}}}{\Lambda}\right)} \cos^2 \theta. \quad (4.50)$$

The characteristic energy of the axions emitted at time  $t$  is given by  $\omega(t) \sim H M_{\text{Pl}}/f$ . Then, we can assume that a particular mass eigenstate effectively stops being emitted when  $\omega(t_{\phi_i}) \approx M_{\phi_i}$  (where we have implicitly defined the time  $t_{\phi_i}$  by this equation), even though the string domain wall network persists long afterwards. This is particularly relevant for the heavier mass eigenstate  $\phi_2$ , as we will see that, for a large part of parameter space, the network disappears long after the strings are unable to produce  $\phi_2$ ,  $t_{\text{ann}} \gg t_{\phi_2} \approx M_{\text{Pl}}/\Lambda^2$ . This is in contrast with the lighter mass eigenstate  $\phi_1$ , for which  $t_{\phi_1} \geq t_{\text{ann}}$  as long as the network annihilates before it dominates the energy density of the universe.

Putting this together, we obtain the total abundance of  $\phi_2$  from strings at present:

$$\begin{aligned} \Omega_{\phi_2, \text{str}}(t_0) &= \frac{n_{\phi_2}(t_{\phi_2}) M_{\phi_2}}{\rho_{c,0}} \left( \frac{R(t_{\phi_2})}{R(t_0)} \right)^3 \\ &\approx c_5 \left( \frac{f}{M_{\text{Pl}}} \right)^{\frac{1}{2}} \frac{\Lambda T_0^3 \cos^2 \theta}{\rho_{c,0}} \\ &= 0.97 \times 10^2 \left( \frac{\Lambda}{10^2 \text{GeV}} \right) \left( \frac{f}{10^{10} \text{GeV}} \right)^{\frac{1}{2}}, \end{aligned} \quad (4.51)$$

where  $c_5 = 0.27 \frac{4}{3} \sqrt{\frac{2}{\pi}} \frac{r_a \alpha}{\sqrt{r\kappa}} \left( \frac{g_{*s0}}{g_{*s}(t_{\phi_2})} \right) \frac{(N_1^2 + N_2^2)^{1/4}}{g_{*s}(t_{\phi_2})^{3/4}}$ .

Now we can calculate the total abundance of the heavy mass eigenstate,  $\phi_2$  by adding the contribution from the domain walls, the strings and from the misalignment mechanism.

We see at once from eqs. 4.41, 4.46 and 4.51, that the heavier mass eigenstate is typically overproduced unless both the instanton scale and the axion decay constant are small. If the string-domain wall network annihilates before dominating the energy density of the universe, the lighter mass eigenstate can be produced by the strings up until the time annihilation of the network. The abundance of  $\phi_1$  is given by:

$$\begin{aligned}\Omega_{\phi_1,\text{str}}(t_0) &= \frac{n_{\phi_1}(t_{\text{ann}})M_{\phi_1}}{\rho_{c,0}} \left( \frac{R(t_{\text{ann}})}{R(t_0)} \right)^3 \\ &\approx c_6 \left( \frac{f}{M_{\text{Pl}}} \right) \frac{\Lambda T_0^3 \sin^2 \theta}{\rho_{c,0} \log \left( \frac{M_{\text{Pl}}}{\Lambda_b} \right)} \\ &= 3.2 \times 10^{-4} \left( \frac{\Lambda}{10^2 \text{GeV}} \right) \left( \frac{f}{10^{10} \text{GeV}} \right),\end{aligned}\tag{4.52}$$

where  $c_6 = 0.76 \frac{4}{3} \sqrt{\frac{2}{\pi}} \frac{r_a \alpha}{\sqrt{r_K}} \left( \frac{g_{*s0}}{g_{*s}(t_{\text{ann}})} \right) \left( \frac{N_2^2 N_b^2 A C_{\text{ann}}}{(N_1^2 + N_2^2) g_{*s}(t_{\text{ann}})^{3/2}} \right)^{\frac{1}{2}}$ . Adding the contributions from misalignment 4.47, the domain walls 4.42, and from the strings 4.52, we conclude that the light mass eigenstate,  $\phi_1$  can constitute the dark matter in the universe. We can see this fact explicitly in fig. 6, which shows the values of  $\Lambda_b$  vs  $f$  for which  $\phi_1$  saturates the observed dark matter abundance. We should keep in mind that we have assumed a standard cosmological evolution throughout, but, as we pointed out earlier, the presence of the heavier mass eigenstate,  $\phi_2$ , can trigger an epoch of early matter domination. However, since an EMD epoch would dilute the abundance of cold  $\phi_1$ s relative to a radiation dominated expansion, we see matter domination can not lead to an overabundance of  $\phi_1$ . We further elaborate on this EMD scenario in App. F, where we show that  $\phi_1$  can saturate the cosmological dark matter abundance also in that case. We, thus, conclude that the abundance of the light axion mass eigenstate resulting from the decay of the network and from the misalignment mechanism can account for the dark matter in the universe.

## 5 Conclusions

In this article, we have explored the phenomenology of axionic string-domain wall networks in the context of string theory. In scenarios containing several axions, as in axiverse constructions, multiple instantons generate a bias term in the potential, which leads to the decay of the network and avoids the domain wall problem.

The decay of the network generates interesting observable signatures, which have been extensively studied in the context of field theory axions. But, an important feature of string theory axion constructions with flat extra dimensions is that the tension of the strings in the network is parametrically larger than for field theory axions. Importantly, this fact can lead to a distinct phenomenology that can enable testing these scenarios in current and forthcoming experiments.

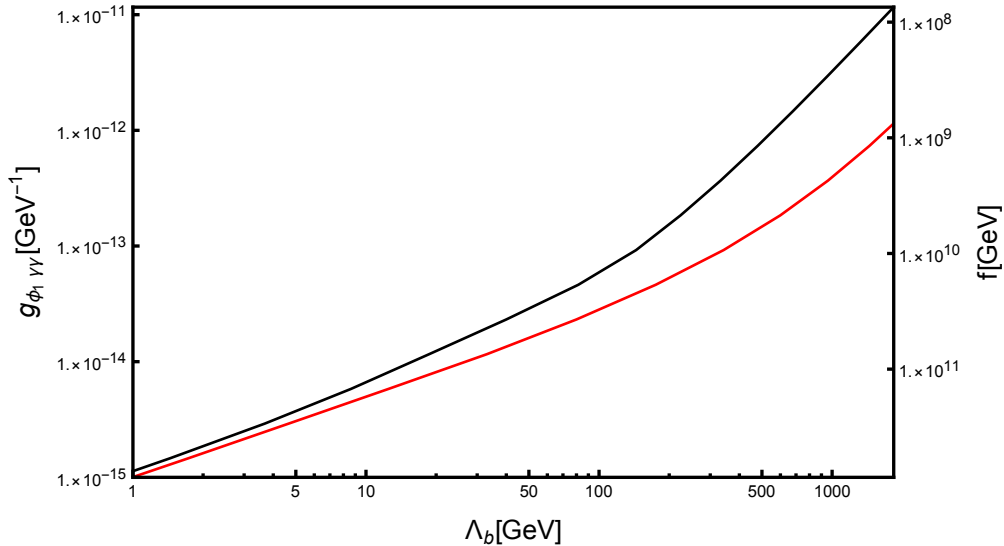


**Figure 6.** The canonical ALP to photon coupling for which the light mass eigenstat  $\phi_1$  can make the entirety of the dark matter. The black (red) curve corresponds to the case of domain walls with an energy density of  $10^{-2}\rho_{\text{tot}}$  ( $10^{-4}\rho_{\text{tot}}$ ) at the time of the annihilation of the network.

For instance, the spectrum of gravitational waves produced by the decay of the network has a characteristic “double peak” structure, that arises because the contribution of the strings in the network, which due to their higher tension cannot be neglected, dominates at higher frequencies. The combined shape of the spectrum is different from the predictions of other early universe phenomena such as phase transitions, field theory axions. Importantly, this singular spectrum provides a telltale sign of string theory axions in gravitational wave observations.

Furthermore, working with a simplified model with two axions, we have shown that the heavier one is typically overproduced. For adequate values of the two-photon coupling, it decays fast enough to avoid conflict with BBN or overclosing the universe. Importantly, the lighter eigenstate can then account for the dark matter in the universe.

Our work is motivated by string theory constructions of axions with flat extra dimensions, and although some of our conclusions might not extend to the case of warped extra dimensions, some might. We have also left aside the study of other interesting phenomenology that could take place in the early universe, such as the production of primordial black holes. These are interesting directions for future work.

## Acknowledgments

We thank J.J. Blanco-Pillado, D. Dunksy, J. Garriga, O. Pujolàs, F. Rompineve and A. Vikman for useful discussions. FF would like to thank the University of the Basque Country (UPV/EHU) for its hospitality during the Cosmological Olentzero Workshop.



## A Condition on the charges

In the main text, we have assumed that the bias potential only couples to the flavor state  $a_1$ :

$$V_b(a_1) = \frac{\Lambda_b^4}{2} \left[ 1 - \cos \left( N_b \frac{a_1}{f_1} \right) \right]. \quad (\text{A.1})$$

However, in general the bias potential can couple to both  $a_1$  and  $a_2$ . Assuming that the two potentials are of the form:

$$V_1(a_1, a_2) = \Lambda^4 \left[ 1 - \cos \left( N_{11} \frac{a_1}{f_1} + N_{12} \frac{a_2}{f_2} \right) \right], \quad (\text{A.2})$$

$$V_2(a_1, a_2) = \Lambda_b^4 \left[ 1 - \cos \left( N_{21} \frac{a_1}{f_1} + N_{22} \frac{a_2}{f_2} \right) \right], \quad (\text{A.3})$$

we can derive the condition for which  $V_2$  allows for a unique minimum [49]. If the charge matrix is invertible, the number of minima of the potential in  $a_1$  is given by”

$$N_{\text{DW}} = \frac{|N_{11}N_{22} - N_{12}N_{21}|}{|\text{gcd}(N_{22}, N_{12})|}. \quad (\text{A.4})$$

We see that, for our choice of values, namely,  $N_{11} = 2$ ,  $N_{12} = N_{21} = 1$  and  $N_{22} = 0$ ,  $N_{\text{DW}} = 1$  where  $\text{gcd}(0, b) = b$  for positive integer  $b$ .

## B Role of unequal initial abundance of vacua

Since the different minima are non completely degenerate, the axion field does not roll down to two nearby minima with equal probability. The true lower energy vacuum is more likely to be populated. This asymmetry in the number of different domain walls acts as a different bias in the network, which can also lead to the annihilation of the string domain wall network. In the case of  $N_{\text{DW}} = 2$  with two non-degenerate minima, the field value has a higher probability of being in the true minimum than in the false minimum at the time of domain wall formation. The ratio of the two probabilities is given by [33]:

$$\frac{p_f}{p_t} = \exp \left( -\frac{\Delta V_b}{V_{\text{min}}} \right), \quad (\text{B.1})$$

where  $p_f$  and  $p_t$  are the probabilities for the field value to fall into the false and true minimum respectively,  $\Delta V_b$  is the difference in potential between the two minima, and  $V_{\text{min}}$  is the minimum value of the leading potential. If we measure the extent of the unequal occupancy by  $p_f = 0.5 - \epsilon$ , the numerical simulations in [35] found:

$$\frac{\tau_{\text{ann}}}{\tau_{\text{form}}} \simeq \epsilon^{-\frac{D}{2}}, \quad (\text{B.2})$$

where  $\tau_{\text{ann}}$  denotes the conformal time of domain wall annihilation,  $\tau_{\text{form}}$  is the conformal time of domain wall formation, and  $D$  is the spatial dimension. Even though, the analysis of [35, 102] considered the specific case of  $N_{\text{DW}} = 2$ , we assume the rate of annihilation is not parametrically faster for the case of  $N_{\text{DW}} > 2$  than eq. B.2. In this case, we have:

$$\frac{\tau_{\text{ann}}}{\tau_{\text{form}}} \simeq \left( \frac{2VN_{\text{DW}}}{\Delta V_b} \right)^3 t_{\text{form}} \frac{3}{2}, \quad (\text{B.3})$$

where we have used  $D = 3$  spatial dimensions. Now we can estimate the typical annihilation timescale associated to the unequal vacuum abundance. During radiation domination,  $\tau \sim \sqrt{t}$ . Parametrically,

$$t_{\text{ann, unequal abundance}} = \left( \frac{2VN_{\text{DW}}}{\Delta V_b} \right)^3 t_{\text{form}} \sim \frac{8N_{\text{DW}}^2 f \Lambda^{10}}{\Lambda_b^{12}}. \quad (\text{B.4})$$

This timescale is much larger than the one associated to the pressure force, which is given in 3.10. Hence, our assumption to just consider the annihilation due to the pressure force is justified.

## C GWs from decays during an early matter dominated era

If the collapse happens during matter domination, the peak amplitude of the GW estimate changes [36]

$$\Omega_{\text{gw}} h^2(t_0) = \Omega_{\text{rad}} h^2 \left( \frac{g_*(T_{\text{reh}})}{g_{*0}} \right) \left( \frac{g_{*s0}}{g_{*s}(T_{\text{reh}})} \right)^{4/3} \left( \frac{H_{\text{reh}}}{H_{\text{ann}}} \right)^{2/3} \Omega_{\text{gw}}(t_{\text{ann}}), \quad (\text{C.1})$$

where  $T_{\text{reh}}$  is the reheating temperature, and  $H_{\text{reh}}$  and  $H_{\text{ann}}$  are the Hubble parameters at  $T = T_{\text{reh}}$  and  $T = T_{\text{ann}}$ , respectively. In the case where the reheating is under perturbative control [139], the Hubble parameter at this stage is of the matter dominated era is given by:

$$H(T) = \left[ \frac{5\pi^2 g_*^2(T)}{72g_*(T_{\text{reh}})} \right]^{1/2} \frac{T^4}{M_P T_{\text{reh}}^2}. \quad (\text{C.2})$$

The peak frequency and the cutoff frequency also change in the following way:

$$f_{\text{peak}} = H(t_{\text{ann}}) \frac{R(t_{\text{ann}})}{R(t_0)} = H(t_{\text{ann}}) \left( \frac{H_{\text{reh}}}{H_{\text{ann}}} \right)^{2/3} \frac{T_{\text{reh}}}{T_0} \quad (\text{C.3})$$

$$f_{\delta} = \delta^{-1} \frac{R(t_{\text{ann}})}{R(t_0)} = \delta^{-1} \left( \frac{H_{\text{reh}}}{H_{\text{ann}}} \right)^{2/3} \frac{T(t_{\text{ann}})}{T_0} \quad (\text{C.4})$$

The resulting spectrum is similar to the standard case shown in fig. 3, but shifted to lower frequencies.

## D Averaged misalignment angle

Assuming that the angular variables  $a_i/f_i$  are uniformly distributed, we get the following for the initial misalignment value of the mass eigenstate:

$$\langle \theta_{2,\text{mis}} \rangle^2 f_{\phi_2}^2 \approx \frac{\pi^2}{3} (f_1 \cos \theta + f_2 \sin \theta)^2, \quad \langle \theta_{1,\text{mis}} \rangle^2 f_{\phi_1}^2 \approx \frac{\pi^2}{3} (f_1 \sin \theta + f_2 \cos \theta)^2, \quad (\text{D.1})$$

However, there are two important subtleties which we glossed over in the main text. Namely, if the initial misalignments of the flavor states are given by  $a_i/f_i = \theta_i$  in a patch of the universe, the displacement of the mass eigenstate is:

$$\phi_2 = a_1 \cos \theta + a_2 \sin \theta = f_1 \theta_1 \cos \theta + f_2 \theta_2 \sin \theta \quad (\text{D.2})$$

Then, the ensemble average assuming a uniform distribution of  $\theta_i$  yields:

$$\begin{aligned} \langle \phi_2^2 \rangle &\equiv \langle \theta_{2,\text{mis}}^2 \rangle f_{\phi_2}^2 \\ &= \frac{\pi^2}{3} (f_1^2 \cos^2 \theta + f_2^2 \sin^2 \theta + 2 \cdot \frac{3}{4} f_1 f_2 \sin \theta \cos \theta) \\ &\neq \frac{\pi^2}{3} (f_1 \cos \theta + f_2 \sin \theta)^2. \end{aligned} \quad (\text{D.3})$$

This has a negligible effect on the total abundance of dark matter when combined with the contribution from the strings and the domain walls. However, a careful analysis of the misalignment mechanism needs to account for the non-uniform initial distribution caused by the time independent axiverse potential, which leads to the fields being more likely to populate the minima of the potential than other values in the field space. We leave this for a future analysis.

## E No EMD from string network decay during scaling

In this section we show that the heavier axion mass eigenstates produced from the strings can only dominate the energy density of the universe close to the annihilation time,  $t_{\text{ann}}$ . The total energy density of the axions produced from the strings in the scaling regime is [49]:

$$\rho_{\phi_2} \approx \frac{16r_a(8\pi)^{3/2}\alpha}{3r^{3/2}\kappa^{3/2}} H^2 \sqrt{f_a M_{\text{pl}}^3} \log \left( \frac{M_{\text{Pl}}}{\Lambda} \right) \cos^2 \theta. \quad (\text{E.1})$$

Assuming that the axions are emitted with a spectrum  $d\dot{E}_a/d\omega \sim 1/\omega$ , the number density of  $\phi_2$  is given by eq. 4.50. Thus, we see that the mean energy of the axions at time  $t$  is given by:

$$\omega_{\phi_i}(t) \approx H(t) \frac{M_{\text{Pl}}}{f} \log^2 \left( \frac{M_{\text{Pl}}}{\Lambda} \right). \quad (\text{E.2})$$

The heavy mass eigenstate production stops before the annihilation of the network [49], at time  $\omega_{\phi_i}(t_{\phi_2}) \approx M_{\phi_2}$ . The  $\phi_2$ 's are non-relativistic at  $t = t_{\phi_2}$ . Hence, the total energy density in  $\phi_2$  at that time is given by:

$$\rho_{\phi_2}(t_{\phi_2}) = n_{\phi_2}(t_{\phi_2})M_{\phi_2} \approx (N_1^2 + N_2^2) \frac{\Lambda^4}{\log^3\left(\frac{M_{\text{Pl}}}{\Lambda}\right)} \sqrt{\frac{f}{M_{\text{Pl}}}}. \quad (\text{E.3})$$

The fractional energy density in  $\phi_2$  at that time is given by:

$$\Omega_{\phi_2}(t_{\phi_2}) = \frac{\rho_{\phi_2}(t_{\phi_2})}{3H(t_{\phi_2})^2 M_{\text{Pl}}^2} \approx \sqrt{\frac{f}{M_{\text{Pl}}}} \frac{\log\left(\frac{M_{\text{Pl}}}{\Lambda}\right)}{3}. \quad (\text{E.4})$$

We, thus, see that at  $t_{\phi_2}$  the universe is not  $\phi_2$  dominated. If the universe is radiation dominated at  $t_{\phi_2}$ , we can evaluate the fractional energy density of  $\phi_2$  at  $t = t_{\text{ann}}$  by assuming the universe remains radiation dominated until  $t_{\text{ann}}$ . We will see that this assumption only breaks down close to  $t = t_{\text{ann}}$ , thus serving as a reasonable approximation. The fractional energy density of  $\phi_2$  at  $t = t_{\text{ann}}$ :

$$\Omega_{\phi_2}(t_{\text{ann}}) \sim \Omega_{\phi_2}(t_{\phi_2}) \sqrt{\frac{t_{\text{ann}}}{t_{\phi_2}}} \sim \frac{f}{M_{\text{Pl}}} \frac{\Lambda^2}{\Lambda_b^2} \log\left(\frac{M_{\text{Pl}}}{\Lambda}\right), \quad (\text{E.5})$$

where we have used eq. 3.10 for  $t_{\text{ann}}$  and eq. E.2 for  $t_{\phi_2}$ . Applying eq. 3.14, so that the domain walls do not dominate the energy density of the universe, we find:

$$\Omega_{\phi_2}(t_{\text{ann}}) < \log\left(\frac{M_{\text{Pl}}}{\Lambda}\right). \quad (\text{E.6})$$

## F Dark matter abundance from EMD

As shown in section 4.2, for the majority of parameter space the heavier eigenstate  $\phi_2$  is overproduced compared to the observed abundance of dark matter. If  $\phi_2$  does not decay immediately, it can lead to a matter dominated era. The total decay width of  $\phi_2$  has large uncertainties due to the model dependence of the couplings to SM fermions. The couplings to other axions are relatively suppressed [111]. As a benchmark, we assume that the decay to photons dominates the total decay. The reheating temperature in that case satisfies:

$$\rho_{\text{tot}}(T_{\text{RH}}) = \frac{\pi^2}{30} g_*(T_{\text{RH}}) T_{\text{RH}}^4 = \frac{4}{3} M_{\text{pl}}^2 \Gamma_{\phi_2\gamma\gamma}^2,$$

where  $\Gamma_{\phi_2\gamma\gamma}$  is given in eq. 4.24. In section 4.2 we noted that, ignoring the EMD, the total abundance of  $\phi_1$  can saturate the observed cosmological dark matter. We now discuss the impact of an EMD on that scenario. The mass of the axion eigenstates is temperature independent. The total energy density in  $\phi_1$  today is given by:

$$\rho_{\phi_1, \text{dw}}(t_0) = \rho_{\phi_1, \text{dw}}(t_{\text{ann}}) \left( \frac{R(t_{\text{ann}})}{R(t_{\text{EMD}})} \right)^3 \left( \frac{R(t_{\text{EMD}})}{R(t_{\text{RH}})} \right)^3 \left( \frac{R(t_{\text{RH}})}{R(t_0)} \right)^3, \quad (\text{F.1})$$

where we have simplified the cosmological evolution by assuming the universe transitions directly from radiation domination to matter domination. Here,  $t_{\text{EMD}}$  denotes the onset of matter domination which can be estimated as follows. The production of  $\phi_2$  from the strings stops before the collapse of the network, as shown in App. E. Assuming that the universe is radiation dominated at this time, the fractional energy density of  $\phi_2$  scales as:

$$\Omega_{\phi_2}(t_{\text{EMD}}) \sim \Omega_{\phi_2}(t_{\phi_2}) \sqrt{\frac{t_{\text{EMD}}}{t_{\phi_2}}} \sim 1. \quad (\text{F.2})$$

The Hubble at the onset of matter domination is:

$$H(t_{\text{EMD}}) \approx \frac{2048\pi\alpha r_a^2}{27\kappa^2 r^2} \frac{f^2}{M_{\text{Pl}}^2} M_{\phi_2}. \quad (\text{F.3})$$

The scale factor during the matter dominated era behaves as:

$$\left( \frac{R(t_{\text{EMD}})}{R(t_{\text{RH}})} \right) = \left( \frac{H(t_{\text{EMD}})}{H(t_{\text{RH}})} \right)^{-\frac{2}{3}}. \quad (\text{F.4})$$

Now we can evaluate the dark matter contribution from the misalignment mechanism. The  $\phi_1$  field starts coherent oscillations when  $M_{\phi_1} \simeq 3H(t_{\text{osc},1})$ . The oscillations start before matter domination:

$$\frac{H(t_{\text{EMD}})}{H(t_{\text{osc},1})} \sim \frac{f^2 \Lambda^2}{M_{\text{Pl}}^2 \Lambda_b^2} < \frac{f}{M_{\text{Pl}}}, \quad (\text{F.5})$$

where in the last part, we have assumed that the bias potential is large enough so that the domain walls annihilate before they dominate the energy density of the universe,  $\Lambda_b > \Lambda \sqrt{f/M_{\text{Pl}}}$ . The total abundance of  $\phi_1$  from the misalignment mechanism is given by:

$$\rho_{\phi_1, \text{mis}}(t_0) = \rho_{\phi_1, \text{mis}}(t_{\text{osc}}) \left( \frac{R(t_{\text{osc}})}{R(t_{\text{EMD}})} \right)^3 \left( \frac{R(t_{\text{EMD}})}{R(t_{\text{RH}})} \right)^3 \left( \frac{R(t_{\text{RH}})}{R(t_0)} \right)^3 \quad (\text{F.6})$$

The contribution from the strings can be calculated similarly by tracking the number density of  $\phi_1$ 's. Assuming that the universe is radiation dominated during the entirety of the network evolution,

$$\rho_{\phi_1, \text{str}}(t_0) = \rho_{\phi_1, \text{str}}(t_{\text{ann}}) \left( \frac{R(t_{\text{ann}})}{R(t_{\text{EMD}})} \right)^3 \left( \frac{R(t_{\text{EMD}})}{R(t_{\text{RH}})} \right)^3 \left( \frac{R(t_{\text{RH}})}{R(t_0)} \right)^3. \quad (\text{F.7})$$

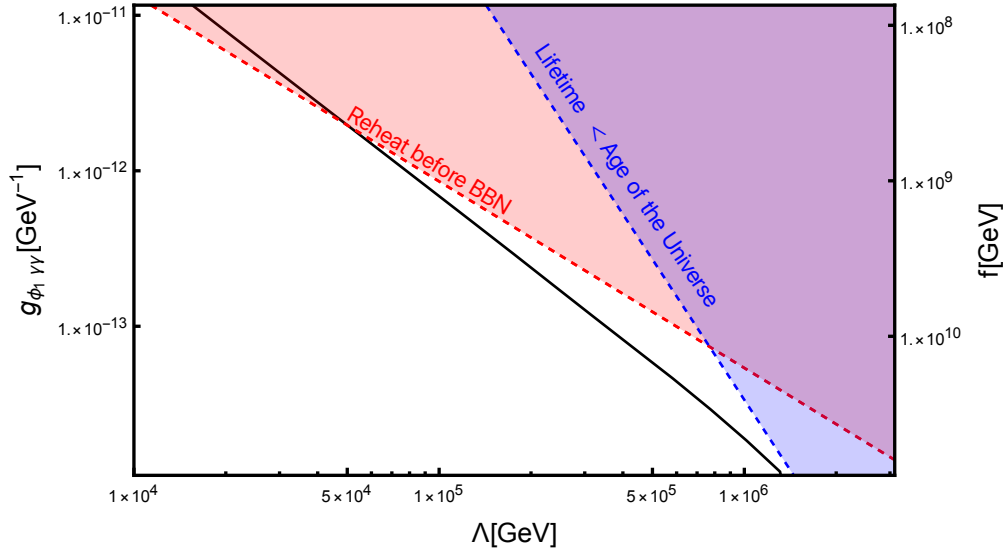


**Figure 7.** The canonical ALP to photon coupling for which the light ALP constitutes the entirety of the dark matter including a period of early matter domination due to  $\phi_2$ . The black curve corresponds to the case of domain walls being  $10^{-1}\rho_{\text{tot}}$  at the time of annihilation of the network. The red dashed line corresponds to a reheating temperature of 5 MeV, allowing conventional BBN. Assuming canonical coupling to photons, are bounds not shown are [114–120].

Hence, the fractional energy density in  $\phi_1$  today is given by

$$\Omega_{\phi_1, \text{tot}}(t_0) = \frac{\rho_{\phi_1, \text{dw}}(t_0) + \rho_{\phi_1, \text{mis}}(t_0) + \rho_{\phi_1, \text{str}}(t_0)}{\rho_{c,0}} \quad (\text{F.8})$$

where  $\rho_{c,0}$  is the critical energy density today. In Fig. 7, we see that  $\phi_1$  can be the entirety of the cosmological dark matter. It should be noted that, although we have assumed a canonical coupling to photons, all of the production mechanisms for the axions are independent of such coupling.

## References

- [1] E. Witten, *Some Properties of  $O(32)$  Superstrings*, *Phys. Lett. B* **149** (1984) 351–356.
- [2] K. Choi and J. E. Kim, *Harmful Axions in Superstring Models*, *Phys. Lett. B* **154** (1985) 393. [Erratum: *Phys.Lett.B* 156, 452 (1985)].
- [3] S. M. Barr, *Harmless Axions in Superstring Theories*, *Phys. Lett. B* **158** (1985) 397–400.
- [4] P. Svrcak and E. Witten, *Axions In String Theory*, *JHEP* **06** (2006) 051, [[hep-th/0605206](#)].
- [5] A. Arvanitaki, S. Dimopoulos, S. Dubovsky, N. Kaloper, and J. March-Russell, *String Axiverse*, *Phys. Rev. D* **81** (2010) 123530, [[arXiv:0905.4720](#)].

- [6] C. A. Baker et al., *An Improved experimental limit on the electric dipole moment of the neutron*, *Phys. Rev. Lett.* **97** (2006) 131801, [[hep-ex/0602020](#)].
- [7] J. M. Pendlebury et al., *Revised experimental upper limit on the electric dipole moment of the neutron*, *Phys. Rev. D* **92** (2015), no. 9 092003, [[arXiv:1509.04411](#)].
- [8] A. Hook, *TASI Lectures on the Strong CP Problem and Axions*, *PoS TASI2018* (2019) 004, [[arXiv:1812.02669](#)].
- [9] R. D. Peccei and H. R. Quinn, *CP Conservation in the Presence of Instantons*, *Phys. Rev. Lett.* **38** (1977) 1440–1443.
- [10] R. D. Peccei and H. R. Quinn, *Constraints Imposed by CP Conservation in the Presence of Instantons*, *Phys. Rev. D* **16** (1977) 1791–1797.
- [11] S. Weinberg, *A New Light Boson?*, *Phys. Rev. Lett.* **40** (1978) 223–226.
- [12] F. Wilczek, *Problem of Strong P and T Invariance in the Presence of Instantons*, *Phys. Rev. Lett.* **40** (1978) 279–282.
- [13] M. Demirtas, N. Gendler, C. Long, L. McAllister, and J. Moritz, *PQ axiverse*, *JHEP* **06** (2023) 092, [[arXiv:2112.04503](#)].
- [14] M. Kamionkowski and J. March-Russell, *Planck scale physics and the Peccei-Quinn mechanism*, *Phys. Lett. B* **282** (1992) 137–141, [[hep-th/9202003](#)].
- [15] S. M. Barr and D. Seckel, *Planck scale corrections to axion models*, *Phys. Rev. D* **46** (1992) 539–549.
- [16] S. Ghigna, M. Lusignoli, and M. Roncadelli, *Instability of the invisible axion*, *Phys. Lett. B* **283** (1992) 278–281.
- [17] H. M. Georgi, L. J. Hall, and M. B. Wise, *Grand Unified Models With an Automatic Peccei-Quinn Symmetry*, *Nucl. Phys. B* **192** (1981) 409–416.
- [18] G. Lazarides, C. Panagiotakopoulos, and Q. Shafi, *Phenomenology and Cosmology With Superstrings*, *Phys. Rev. Lett.* **56** (1986) 432.
- [19] R. Holman, S. D. H. Hsu, T. W. Kephart, E. W. Kolb, R. Watkins, and L. M. Widrow, *Solutions to the strong CP problem in a world with gravity*, *Phys. Lett. B* **282** (1992) 132–136, [[hep-ph/9203206](#)].
- [20] S.-Y. Ho, K. Saikawa, and F. Takahashi, *Enhanced photon coupling of ALP dark matter adiabatically converted from the QCD axion*, *JCAP* **10** (2018) 042, [[arXiv:1806.09551](#)].
- [21] F. Chadha-Day, *Axion-like particle oscillations*, *JCAP* **01** (2022), no. 01 013, [[arXiv:2107.12813](#)].
- [22] J. W. Foster, S. Kumar, B. R. Safdi, and Y. Soreq, *Dark Grand Unification in the axiverse: decaying axion dark matter and spontaneous baryogenesis*, *JHEP* **12** (2022) 119, [[arXiv:2208.10504](#)].
- [23] K. Murai, F. Takahashi, and W. Yin, *QCD axion: A unique player in the axiverse with mixings*, *Phys. Rev. D* **108** (2023), no. 3 036020, [[arXiv:2305.18677](#)].
- [24] G. R. Dvali and S. H. H. Tye, *Brane inflation*, *Phys. Lett. B* **450** (1999) 72–82, [[hep-ph/9812483](#)].

- [25] N. T. Jones, H. Stoica, and S. H. H. Tye, *Brane interaction as the origin of inflation*, *JHEP* **07** (2002) 051, [[hep-th/0203163](#)].
- [26] A. R. Frey, A. Mazumdar, and R. C. Myers, *Stringy effects during inflation and reheating*, *Phys. Rev. D* **73** (2006) 026003, [[hep-th/0508139](#)].
- [27] S. Sarangi and S. H. H. Tye, *Cosmic string production towards the end of brane inflation*, *Phys. Lett. B* **536** (2002) 185–192, [[hep-th/0204074](#)].
- [28] T. C. Bachlechner, K. Eckerle, O. Janssen, and M. Kleban, *Multiple-axion framework*, *Phys. Rev. D* **98** (2018), no. 6 061301, [[arXiv:1703.00453](#)].
- [29] D. Hu, H.-R. Jiang, H.-L. Li, M.-L. Xiao, and J.-H. Yu, *Tale of two-  $U(1)$  axion models*, *Phys. Rev. D* **103** (2021), no. 9 095025, [[arXiv:2009.01452](#)].
- [30] P. Sikivie, *Of Axions, Domain Walls and the Early Universe*, *Phys. Rev. Lett.* **48** (1982) 1156–1159.
- [31] Y. B. Zeldovich, I. Y. Kobzarev, and L. B. Okun, *Cosmological Consequences of the Spontaneous Breakdown of Discrete Symmetry*, *Zh. Eksp. Teor. Fiz.* **67** (1974) 3–11.
- [32] T. Hiramatsu, M. Kawasaki, K. Saikawa, and T. Sekiguchi, *Axion cosmology with long-lived domain walls*, *JCAP* **01** (2013) 001, [[arXiv:1207.3166](#)].
- [33] T. Hiramatsu, M. Kawasaki, and K. Saikawa, *Evolution of String-Wall Networks and Axionic Domain Wall Problem*, *JCAP* **08** (2011) 030, [[arXiv:1012.4558](#)].
- [34] T. W. B. Kibble, *Topology of Cosmic Domains and Strings*, *J. Phys. A* **9** (1976) 1387–1398.
- [35] S. E. Larsson, S. Sarkar, and P. L. White, *Evading the cosmological domain wall problem*, *Phys. Rev. D* **55** (1997) 5129–5135, [[hep-ph/9608319](#)].
- [36] K. Saikawa, *A review of gravitational waves from cosmic domain walls*, *Universe* **3** (2017), no. 2 40, [[arXiv:1703.02576](#)].
- [37] Y. Bai, T.-K. Chen, and M. Korwar, *QCD-collapsed domain walls: QCD phase transition and gravitational wave spectroscopy*, *JHEP* **12** (2023) 194, [[arXiv:2306.17160](#)].
- [38] Y. Gouttenoire, S. F. King, R. Roshan, X. Wang, G. White, and M. Yamazaki, *Cosmological Consequences of Domain Walls Biased by Quantum Gravity*, [arXiv:2501.16414](#).
- [39] A. Vilenkin and A. E. Everett, *Cosmic Strings and Domain Walls in Models with Goldstone and PseudoGoldstone Bosons*, *Phys. Rev. Lett.* **48** (1982) 1867–1870.
- [40] A. Vilenkin, *Cosmic Strings and Domain Walls*, *Phys. Rept.* **121** (1985) 263–315.
- [41] R. L. Davis, *Cosmic Axions from Cosmic Strings*, *Phys. Lett. B* **180** (1986) 225–230.
- [42] G. R. Vincent, M. Hindmarsh, and M. Sakellariadou, *Scaling and small scale structure in cosmic string networks*, *Phys. Rev. D* **56** (1997) 637–646, [[astro-ph/9612135](#)].
- [43] A. R. Zhitnitsky, *On Possible Suppression of the Axion Hadron Interactions. (In Russian)*, *Sov. J. Nucl. Phys.* **31** (1980) 260.
- [44] M. Dine, W. Fischler, and M. Srednicki, *A Simple Solution to the Strong CP Problem with a Harmless Axion*, *Phys. Lett. B* **104** (1981) 199–202.



- [45] F. Iocco, G. Mangano, G. Miele, O. Pisanti, and P. D. Serpico, *Primordial Nucleosynthesis: from precision cosmology to fundamental physics*, *Phys. Rept.* **472** (2009) 1–76, [[arXiv:0809.0631](#)].
- [46] W. H. Zurek, *Cosmological Experiments in Superfluid Helium?*, *Nature* **317** (1985) 505–508.
- [47] E. J. Copeland, R. C. Myers, and J. Polchinski, *Cosmic F and D strings*, *JHEP* **06** (2004) 013, [[hep-th/0312067](#)].
- [48] M. Cicoli, A. Hebecker, J. Jaeckel, and M. Wittner, *Axions in string theory — slaying the Hydra of dark radiation*, *JHEP* **09** (2022) 198, [[arXiv:2203.08833](#)].
- [49] J. N. Benabou, Q. Bonnefoy, M. Buschmann, S. Kumar, and B. R. Safdi, *The Cosmological Dynamics of String Theory Axion Strings*, [arXiv:2312.08425](#).
- [50] T. C. Bachlechner, C. Long, and L. McAllister, *Planckian Axions and the Weak Gravity Conjecture*, *JHEP* **01** (2016) 091, [[arXiv:1503.07853](#)].
- [51] P. Sikivie, *Axion Cosmology*, *Lect. Notes Phys.* **741** (2008) 19–50, [[astro-ph/0610440](#)].
- [52] D. Harlow and H. Ooguri, *Symmetries in quantum field theory and quantum gravity*, *Commun. Math. Phys.* **383** (2021), no. 3 1669–1804, [[arXiv:1810.05338](#)].
- [53] M. Reece, *TASI Lectures: (No) Global Symmetries to Axion Physics*, *PoS TASI2022* (2024) 008, [[arXiv:2304.08512](#)].
- [54] T. Hiramatsu, M. Kawasaki, and K. Saikawa, *Gravitational Waves from Collapsing Domain Walls*, *JCAP* **05** (2010) 032, [[arXiv:1002.1555](#)].
- [55] M. Kawasaki and K. Saikawa, *Study of gravitational radiation from cosmic domain walls*, *JCAP* **09** (2011) 008, [[arXiv:1102.5628](#)].
- [56] T. Hiramatsu, M. Kawasaki, and K. Saikawa, *On the estimation of gravitational wave spectrum from cosmic domain walls*, *JCAP* **02** (2014) 031, [[arXiv:1309.5001](#)].
- [57] R. Zambujal Ferreira, A. Notari, O. Pujolàs, and F. Rompineve, *High Quality QCD Axion at Gravitational Wave Observatories*, *Phys. Rev. Lett.* **128** (2022), no. 14 141101, [[arXiv:2107.07542](#)].
- [58] N. Kitajima, J. Lee, K. Murai, F. Takahashi, and W. Yin, *Gravitational waves from domain wall collapse, and application to nanohertz signals with QCD-coupled axions*, *Phys. Lett. B* **851** (2024) 138586, [[arXiv:2306.17146](#)].
- [59] R. Z. Ferreira, S. Gasparotto, T. Hiramatsu, I. Obata, and O. Pujolas, *Axionic defects in the CMB: birefringence and gravitational waves*, *JCAP* **05** (2024) 066, [[arXiv:2312.14104](#)].
- [60] **KAGRA, Virgo, LIGO Scientific** Collaboration, R. Abbott et al., *Upper limits on the isotropic gravitational-wave background from Advanced LIGO and Advanced Virgo’s third observing run*, *Phys. Rev. D* **104** (2021), no. 2 022004, [[arXiv:2101.12130](#)].
- [61] **NANOGrav** Collaboration, G. Agazie et al., *The NANOGrav 15 yr Data Set: Evidence for a Gravitational-wave Background*, *Astrophys. J. Lett.* **951** (2023), no. 1 L8, [[arXiv:2306.16213](#)].
- [62] H. Xu et al., *Searching for the Nano-Hertz Stochastic Gravitational Wave Background with the Chinese Pulsar Timing Array Data Release I*, *Res. Astron. Astrophys.* **23** (2023), no. 7 075024, [[arXiv:2306.16216](#)].

- [63] A. Weltman et al., *Fundamental physics with the Square Kilometre Array*, *Publ. Astron. Soc. Austral.* **37** (2020) e002, [[arXiv:1810.02680](#)].
- [64] **LISA** Collaboration, P. Amaro-Seoane et al., *Laser Interferometer Space Antenna*, [arXiv:1702.00786](#).
- [65] G. M. Harry, P. Fritschel, D. A. Shaddock, W. Folkner, and E. S. Phinney, *Laser interferometry for the big bang observer*, *Class. Quant. Grav.* **23** (2006) 4887–4894. [Erratum: *Class.Quant.Grav.* **23**, 7361 (2006)].
- [66] S. Kawamura et al., *Current status of space gravitational wave antenna DECIGO and B-DECIGO*, *PTEP* **2021** (2021), no. 5 05A105, [[arXiv:2006.13545](#)].
- [67] M. Maggiore et al., *Science Case for the Einstein Telescope*, *JCAP* **03** (2020) 050, [[arXiv:1912.02622](#)].
- [68] **TianQin** Collaboration, J. Luo et al., *TianQin: a space-borne gravitational wave detector*, *Class. Quant. Grav.* **33** (2016), no. 3 035010, [[arXiv:1512.02076](#)].
- [69] W.-H. Ruan, Z.-K. Guo, R.-G. Cai, and Y.-Z. Zhang, *Taiji program: Gravitational-wave sources*, *Int. J. Mod. Phys. A* **35** (2020), no. 17 2050075, [[arXiv:1807.09495](#)].
- [70] D. Reitze et al., *Cosmic Explorer: The U.S. Contribution to Gravitational-Wave Astronomy beyond LIGO*, *Bull. Am. Astron. Soc.* **51** (2019), no. 7 035, [[arXiv:1907.04833](#)].
- [71] J. Crowder and N. J. Cornish, *Beyond LISA: Exploring future gravitational wave missions*, *Phys. Rev. D* **72** (2005) 083005, [[gr-qc/0506015](#)].
- [72] G. Janssen et al., *Gravitational wave astronomy with the SKA*, *PoS AASKA14* (2015) 037, [[arXiv:1501.00127](#)].
- [73] L. M. Widrow, *The Collapse of Nearly Spherical Domain Walls*, *Phys. Rev. D* **39** (1989) 3576.
- [74] F. Ferrer, E. Masso, G. Panico, O. Pujolas, and F. Rompineve, *Primordial Black Holes from the QCD axion*, *Phys. Rev. Lett.* **122** (2019), no. 10 101301, [[arXiv:1807.01707](#)].
- [75] G. B. Gelmini, A. Simpson, and E. Vitagliano, *Catastrogenesis: DM, GWs, and PBHs from ALP string-wall networks*, *JCAP* **02** (2023) 031, [[arXiv:2207.07126](#)].
- [76] D. I. Dunskey and M. Kongsore, *Primordial Black Holes from Axion Domain Wall Collapse*, [arXiv:2402.03426](#).
- [77] M. Kawasaki, K. Saikawa, and T. Sekiguchi, *Axion dark matter from topological defects*, *Phys. Rev. D* **91** (2015), no. 6 065014, [[arXiv:1412.0789](#)].
- [78] K. Harigaya and M. Kawasaki, *QCD axion dark matter from long-lived domain walls during matter domination*, *Phys. Lett. B* **782** (2018) 1–5, [[arXiv:1802.00579](#)].
- [79] J. M. Cline, C. Litos, and W. Xue, *Axion strings from string axions*, [arXiv:2412.12260](#).
- [80] A. Sen, *Non-BPS D-branes in string theory*, *Class. Quant. Grav.* **17** (2000) 1251–1256.
- [81] G. Dvali and A. Vilenkin, *Solitonic D-branes and brane annihilation*, *Phys. Rev. D* **67** (2003) 046002, [[hep-th/0209217](#)].
- [82] J. J. Blanco-Pillado, G. Dvali, and M. Redi, *Cosmic D-strings as axionic D-term strings*, *Phys. Rev. D* **72** (2005) 105002, [[hep-th/0505172](#)].

- [83] P. P. Avelino, C. J. A. P. Martins, and J. C. R. E. Oliveira, *One-scale model for domain wall network evolution*, *Phys. Rev. D* **72** (2005) 083506, [[hep-ph/0507272](#)].
- [84] P. P. Avelino, C. J. A. P. Martins, J. Menezes, R. Menezes, and J. C. R. E. Oliveira, *Dynamics of domain wall networks with junctions*, *Phys. Rev. D* **78** (2008) 103508, [[arXiv:0807.4442](#)].
- [85] M. Kuster, G. Raffelt, and B. Beltran, eds., *Axions: Theory, cosmology, and experimental searches. Proceedings, 1st Joint ILIAS-CERN-CAST axion training, Geneva, Switzerland, November 30-December 2, 2005*, vol. 741, 2008.
- [86] T. Hiramatsu, M. Kawasaki, K. Saikawa, and T. Sekiguchi, *Production of dark matter axions from collapse of string-wall systems*, *Phys. Rev. D* **85** (2012) 105020, [[arXiv:1202.5851](#)]. [Erratum: *Phys.Rev.D* 86, 089902 (2012)].
- [87] M. Yamaguchi, M. Kawasaki, and J. Yokoyama, *Evolution of axionic strings and spectrum of axions radiated from them*, *Phys. Rev. Lett.* **82** (1999) 4578–4581, [[hep-ph/9811311](#)].
- [88] M. Yamaguchi and J. Yokoyama, *Quantitative evolution of global strings from the Lagrangian view point*, *Phys. Rev. D* **67** (2003) 103514, [[hep-ph/0210343](#)].
- [89] M. Yamaguchi and J. Yokoyama, *Lagrangian evolution of global strings*, *Phys. Rev. D* **66** (2002) 121303, [[hep-ph/0205308](#)].
- [90] J. March-Russell and H. Tillim, *Axiverse Strings*, [arXiv:2109.14637](#).
- [91] M. J. Dolan, P. Draper, J. Kozaczuk, and H. Patel, *Transplanckian Censorship and Global Cosmic Strings*, *JHEP* **04** (2017) 133, [[arXiv:1701.05572](#)].
- [92] M. Reece, *Photon Masses in the Landscape and the Swampland*, *JHEP* **07** (2019) 181, [[arXiv:1808.09966](#)].
- [93] S. Lanza, F. Marchesano, L. Martucci, and I. Valenzuela, *The EFT stringy viewpoint on large distances*, *JHEP* **09** (2021) 197, [[arXiv:2104.05726](#)].
- [94] B. Heidenreich, M. Reece, and T. Rudelius, *The Weak Gravity Conjecture and axion strings*, *JHEP* **11** (2021) 004, [[arXiv:2108.11383](#)].
- [95] J. J. Blanco-Pillado, K. D. Olum, and B. Shlaer, *The number of cosmic string loops*, *Phys. Rev. D* **89** (2014), no. 2 023512, [[arXiv:1309.6637](#)].
- [96] C. Ringeval, M. Sakellariadou, and F. Bouchet, *Cosmological evolution of cosmic string loops*, *JCAP* **02** (2007) 023, [[astro-ph/0511646](#)].
- [97] L. Lorenz, C. Ringeval, and M. Sakellariadou, *Cosmic string loop distribution on all length scales and at any redshift*, *JCAP* **10** (2010) 003, [[arXiv:1006.0931](#)].
- [98] T. Vachaspati and A. Vilenkin, *Gravitational radiation from cosmic strings*, *Phys. Rev. D* **31** (Jun, 1985) 3052–3058.
- [99] B. Allen and E. P. S. Shellard, *Gravitational radiation from cosmic strings*, *Phys. Rev. D* **45** (1992) 1898–1912.
- [100] B. Allen and P. Casper, *A Closed form expression for the gravitational radiation rate from cosmic strings*, *Phys. Rev. D* **50** (1994) 2496–2518, [[gr-qc/9405005](#)].
- [101] C. J. A. P. Martins, I. Y. Rybak, A. Avgoustidis, and E. P. S. Shellard, *Extending the*

- velocity-dependent one-scale model for domain walls*, *Phys. Rev. D* **93** (2016), no. 4 043534, [[arXiv:1602.01322](#)].
- [102] D. Coulson, Z. Lalak, and B. A. Ovrut, *Biased domain walls*, *Phys. Rev. D* **53** (1996) 4237–4246.
- [103] R. Z. Ferreira, A. Notari, O. Pujolàs, and F. Rompineve, *Collapsing domain wall networks: impact on pulsar timing arrays and primordial black holes*, *JCAP* **06** (2024) 020, [[arXiv:2401.14331](#)].
- [104] M. Maggiore, *Gravitational Waves: Volume 1: Theory and Experiments*. Oxford University Press, 10, 2007.
- [105] C. Caprini and D. G. Figueroa, *Cosmological Backgrounds of Gravitational Waves*, *Class. Quant. Grav.* **35** (2018), no. 16 163001, [[arXiv:1801.04268](#)].
- [106] R.-G. Cai, S. Pi, and M. Sasaki, *Universal infrared scaling of gravitational wave background spectra*, *Phys. Rev. D* **102** (2020), no. 8 083528, [[arXiv:1909.13728](#)].
- [107] K. Saikawa and S. Shirai, *Primordial gravitational waves, precisely: The role of thermodynamics in the Standard Model*, *JCAP* **05** (2018) 035, [[arXiv:1803.01038](#)].
- [108] R. L. Davis, *Goldstone Bosons in String Models of Galaxy Formation*, *Phys. Rev. D* **32** (1985) 3172.
- [109] A. Vilenkin and T. Vachaspati, *Radiation of Goldstone Bosons From Cosmic Strings*, *Phys. Rev. D* **35** (1987) 1138.
- [110] P. Auclair et al., *Probing the gravitational wave background from cosmic strings with LISA*, *JCAP* **04** (2020) 034, [[arXiv:1909.00819](#)].
- [111] N. Gendler, D. J. E. Marsh, L. McAllister, and J. Moritz, *Glimmers from the Axiverse*, [[arXiv:2309.13145](#)].
- [112] D. Aloni, Y. Soreq, and M. Williams, *Coupling QCD-Scale Axionlike Particles to Gluons*, *Phys. Rev. Lett.* **123** (2019), no. 3 031803, [[arXiv:1811.03474](#)].
- [113] B. Gavela, P. Quílez, and M. Ramos, *The QCD axion sum rule*, *JHEP* **04** (2024) 056, [[arXiv:2305.15465](#)].
- [114] J. Jaeckel, P. C. Malta, and J. Redondo, *Decay photons from the axionlike particles burst of type II supernovae*, *Phys. Rev. D* **98** (2018), no. 5 055032, [[arXiv:1702.02964](#)].
- [115] S. Hoof and L. Schulz, *Updated constraints on axion-like particles from temporal information in supernova SN1987A gamma-ray data*, *JCAP* **03** (2023) 054, [[arXiv:2212.09764](#)].
- [116] E. Müller, F. Calore, P. Carena, C. Eckner, and M. C. D. Marsh, *Investigating the gamma-ray burst from decaying MeV-scale axion-like particles produced in supernova explosions*, *JCAP* **07** (2023) 056, [[arXiv:2304.01060](#)].
- [117] S. Porras-Bedmar, M. Meyer, and D. Horns, *Novel bounds on decaying axionlike particle dark matter from the cosmic background*, *Phys. Rev. D* **110** (7, 2024) 103501, [[arXiv:2407.10618](#)].
- [118] A. Ayala, I. Domínguez, M. Giannotti, A. Mirizzi, and O. Straniero, *Revisiting the bound on axion-photon coupling from Globular Clusters*, *Phys. Rev. Lett.* **113** (2014), no. 19 191302, [[arXiv:1406.6053](#)].

- [119] M. J. Dolan, F. J. Hiskens, and R. R. Volkas, *Advancing globular cluster constraints on the axion-photon coupling*, *JCAP* **10** (2022) 096, [[arXiv:2207.03102](#)].
- [120] D. Cadamuro and J. Redondo, *Cosmological bounds on pseudo Nambu-Goldstone bosons*, *JCAP* **02** (2012) 032, [[arXiv:1110.2895](#)].
- [121] M. S. Turner, *Cosmic and Local Mass Density of Invisible Axions*, *Phys. Rev. D* **33** (1986) 889–896.
- [122] D. H. Lyth, *Axions and inflation: Sitting in the vacuum*, *Phys. Rev. D* **45** (1992) 3394–3404.
- [123] K. Strobl and T. J. Weiler, *Anharmonic evolution of the cosmic axion density spectrum*, *Phys. Rev. D* **50** (1994) 7690–7702, [[astro-ph/9405028](#)].
- [124] T. Kobayashi, R. Kurematsu, and F. Takahashi, *Isocurvature Constraints and Anharmonic Effects on QCD Axion Dark Matter*, *JCAP* **09** (2013) 032, [[arXiv:1304.0922](#)].
- [125] K. J. Bae, J.-H. Huh, and J. E. Kim, *Update of axion CDM energy*, *JCAP* **09** (2008) 005, [[arXiv:0806.0497](#)].
- [126] L. Visinelli and P. Gondolo, *Dark Matter Axions Revisited*, *Phys. Rev. D* **80** (2009) 035024, [[arXiv:0903.4377](#)].
- [127] D. Harari and P. Sikivie, *On the Evolution of Global Strings in the Early Universe*, *Phys. Lett. B* **195** (1987) 361–365.
- [128] C. Hagmann and P. Sikivie, *Computer simulations of the motion and decay of global strings*, *Nucl. Phys. B* **363** (1991) 247–280.
- [129] R. L. Davis and E. P. S. Shellard, *DO AXIONS NEED INFLATION?*, *Nucl. Phys. B* **324** (1989) 167–186.
- [130] R. A. Battye and E. P. S. Shellard, *Global string radiation*, *Nucl. Phys. B* **423** (1994) 260–304, [[astro-ph/9311017](#)].
- [131] R. A. Battye and E. P. S. Shellard, *Axion string constraints*, *Phys. Rev. Lett.* **73** (1994) 2954–2957, [[astro-ph/9403018](#)]. [Erratum: *Phys.Rev.Lett.* 76, 2203–2204 (1996)].
- [132] E. P. S. Shellard, *Cosmic String Interactions*, *Nucl. Phys. B* **283** (1987) 624–656.
- [133] V. B. . Klaer and G. D. Moore, *The dark-matter axion mass*, *JCAP* **11** (2017) 049, [[arXiv:1708.07521](#)].
- [134] A. Vaquero, J. Redondo, and J. Stadler, *Early seeds of axion miniclusters*, *JCAP* **04** (2019) 012, [[arXiv:1809.09241](#)].
- [135] M. Gorghetto, E. Hardy, and G. Villadoro, *Axions from Strings: the Attractive Solution*, *JHEP* **07** (2018) 151, [[arXiv:1806.04677](#)].
- [136] M. Gorghetto, E. Hardy, and G. Villadoro, *More axions from strings*, *SciPost Phys.* **10** (2021), no. 2 050, [[arXiv:2007.04990](#)].
- [137] M. Buschmann, J. W. Foster, and B. R. Safdi, *Early-Universe Simulations of the Cosmological Axion*, *Phys. Rev. Lett.* **124** (2020), no. 16 161103, [[arXiv:1906.00967](#)].
- [138] M. Buschmann, J. W. Foster, A. Hook, A. Peterson, D. E. Willcox, W. Zhang, and B. R. Safdi, *Dark matter from axion strings with adaptive mesh refinement*, *Nature Commun.* **13** (2022), no. 1 1049, [[arXiv:2108.05368](#)].

- [139] G. F. Giudice, E. W. Kolb, and A. Riotto, *Largest temperature of the radiation era and its cosmological implications*, *Phys. Rev. D* **64** (2001) 023508, [[hep-ph/0005123](#)].